Int. J. Electrochem. Sci., 9 **(2014)** 5607 - 5639

International Journal of
ELECTROCHEMICAL
SCIENCE
www.electrochemsci.org

Review

Review: An Overview of Recent Development of Platinum-Based Cathode Materials for Direct Methanol Fuel Cells

R.N. Singh[*], *R. Awasthi and C.S. Sharma*

Department of Chemistry, Centre of Advanced Study, Banaras Hindu University, Varanasi-221 005, India
[*]E-mail: rnsbhu@rediffmail.com & rnsbhu@gmail.com

Received: 1 April 2014 / *Accepted:* 10 June 2014 / *Published:* 16 July 2014

Among pure metals, platinum is the best electrocatalyst for the oxygen reduction reaction (ORR) in direct methanol fuel cells. Its activity is further improved when supported on a high surface area carbon support. However, platinum metal is pretty costly and highly sensitive to the presence of even small amounts of liquid fuel that permeates from anode to the cathode side through the commonly used Nafion electrolyte membrane. Concerted efforts have been made to improve its methanol tolerance and mass utilization efficiency. As a result, several novel bi- and multi-metallic Pt alloys/composites and other Pt-based electrodes with innovative designs, such as hollow Pt nano-spheres, core/shell Pt/C nanoparticles, Pt-rich (or pure) skin structure, etc. have recently been reported. This paper presents an overview of all the advances made with regard to design, synthesis and ORR activity of Pt-based cathodes during the period 2000-2013.

Keywords: Direct Alcohol Fuel Cells, Oxygen Reduction Reaction, Nanoparticles, Core-Shell Electrocatalysts, Nanocomposites.

1. INTRODUCTION

Low temperature fuel cells, with either hydrogen or alcohol as the fuel, represent an environmentally friendly technology and are attracting considerable interest as a means of producing electricity by direct electrochemical conversion of hydrogen/alcohol and oxygen into water/water and carbon dioxide [1-3]. Among direct alcohol fuel cells (DAFCs), direct methanol fuel cells (DMFCs) have received the most extensive attention [1-8]. Besides methanol (Energy Density, E.D. = 6.09 kWh/kg, b. p. 64.7 ºC), several other small organic molecules, such as ethanol (E.D. = 8.00 $kWhkg^{-1}$, b. p. 78.4 ºC) [2-6, 9], 2-propanol (E.D. = 8.58 $kWhkg^{-1}$, b. p. 82.5 ºC) [4-6, 10], ethylene glycol (EG) (E.D. = 5.2 $kWhkg^{-1}$, b. p. 197.3 ºC) [4-6, 11], and formic acid (FA) (E.D. = 2.086 $kWhL^{-1}$, b. p.

100.8 ºC) [12-13] have also received attention as typical fuel alternatives because of their higher energy densities, and lower volatility and toxicity than methanol. In DMFCs, Pt and Pt-based alloys are used as the most active cathode materials for the oxygen reduction reaction (ORR) both in acid as well as in alkaline solutions. However, platinum metal is pretty costly and less abundant on the earth [14]. Also, it is highly sensitive to the presence of even a small amount of liquid fuels and/or reaction intermediates that permeate from anode to the cathode side through the commonly used Nafion electrolyte membrane [15]. During the discharge of a DMFC through the cathodic ($O_2 + 4H^+ + 4e^- \rightarrow 2H_2O$) and anodic ($CH_3OH + H_2O \rightarrow CO_2 + 6H^+ + 6e^-$) reactions, the CH_3OH molecule dissolved in the electrolyte can migrate towards the cathode through the polymer electrolyte membrane (methanol crossover) where it is oxidized, the standard potential of the CO_2/CH_3OH couple being 0.016 V/SHE << 1.23 V/SHE (the standard potential of the O_2/H_2O couple). So, such a fuel crossover not only lowers the fuel utilization, but also degrades the cathode performance (excess cathode polarization), resulting in a significant decrease of the cathode potential and thus of the cell voltage. Compared to methanol, ethanol, 2-propanol, EG and FA are less prone to crossover, but their influence on the cathode performance is not negligible [16-19]. This is a serious drawback of the DMFC, unless the cathode material is inactive toward the methanol oxidation reaction (MOR). To minimize the adverse effect of methanol crossover and reduce the cost of cathode, researches have been carried out mainly in two directions: (i) design and synthesis of Pt-based cathode materials with both higher methanol tolerance and higher activity for the ORR than Pt and (ii) search for novel methanol tolerance and corrosion stable non-Pt cathode materials with activity comparable to Pt. With the aim to decrease the Pt loading and improve the ORR kinetics several new classes of the Pt based ORR catalysts such as Pt-based binary and ternary alloys/ nanocomposites [20, 21], Pt catalysts with core-shell structures [22], Pt bi-metals and alloys with hollow and porous nanostructures [23], Pt-on-M (M = metal) hetero nanostructures or nanodentrites [24], etc. have recently been reported. Several non-precious materials [25], such as first row transition metal chalcogenides (oxides [26], sulphides [27], and selenides [15]), transition metals macrocycles [28], transition metal mixed oxide (s) and graphene hybrids [29-30], Pd-based composites/alloys [31-33], etc. [34], have also been discovered as active ORR catalysts. To avoid complexities and voluminous presentation, only Pt or Pt-based materials investigated as active cathodes for the ORR during recent years (i.e. from 2000 to till date) are briefly discussed in this report with the aim to provide relevant and concise information on recent technological developments in the area concerned.

1.1 Oxygen reduction reaction (ORR)

The ORR is the primary electrochemical reaction occurring at the cathode of the fuel cells. The ORR can follow the following two mechanistic paths [35]:

(i) The direct $4e^-$ transfer mechanism:

(a) In alkaline solutions,

$$O_2 + 2H_2O + 4e^- \rightarrow 4OH^- \qquad (E^\circ = 0.4\ V\ vs.\ SHE)$$

(b) In acidic solutions,

$$O_2 + 4H^+ + 4e^- \rightarrow 2H_2O \qquad (E^\circ = 1.229\ V\ vs.SHE)$$

(ii) The $2e^-$ transfer mechanism or the peroxide path.

(a) In alkaline solutions,

$$O_2 + H_2O + 2e^- \rightarrow HO_2^- + OH^- \qquad (E^\circ = -0.07\ V\ vs.SHE)$$

$$HO_2^- + H_2O + 2e^- \rightarrow 3OH^- \qquad (E^\circ = 0.87\ V\ vs.SHE)$$

(b) In acid solutions,

$$O_2 + 2H^+ + 2e^- \rightarrow H_2O_2 \qquad (E^\circ = 0.67\ V\ vs.SHE)$$

$$H_2O_2 + 2H^+ + 2e^- \rightarrow 2H_2O \qquad (E^\circ = 1.77\ V\ vs.SHE)$$

The direct $4e^-$ oxygen reduction path is more efficient than $2e^-$ reduction path. The generalized scheme for the ORR represented by Wroblowa et al. [36] is shown in Figure 1.

where, k_1 = rate constant for $4e^-$ direct reduction to H_2O or OH-

k_2= $2e^-$ reduction to H_2O_2 or HO_2^-

k_3 = electrochemical reduction of H_2O_2 to water or OH^-

k_4 = catalytic decomposition of H_2O_2 or HO_2^- yielding reducible product

k_5 = desorption of adsorbed H_2O_2 or HO_2^-

k_6 = adsorption of H_2O_2 or HO_2^-

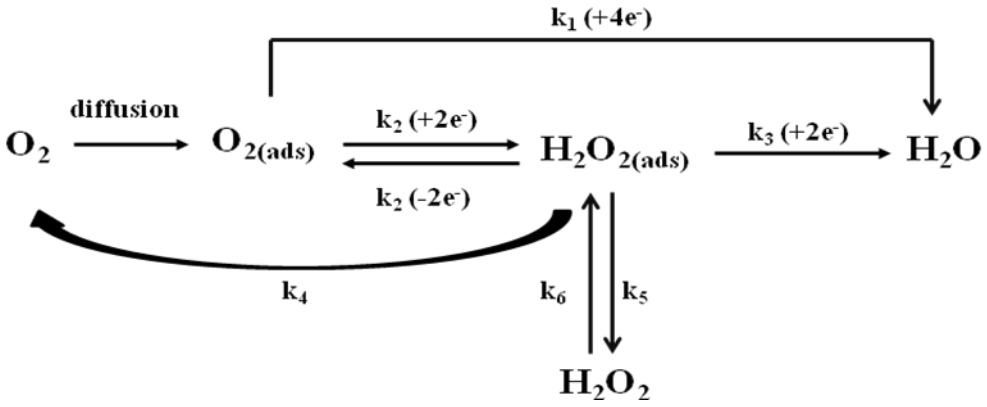

Figure 1. Schematic presentation of ORR pathway.

At high potentials k_1/k_2 is constant with $k_1>k_2$ indicating a direct reduction of oxygen to water. At intermediate potentials, k_1/k_2 ratio decreases indicating an increase in the $2e^-$ reduction of oxygen to peroxide. At lower potentials, k_1/k_2 becomes lower than 1. However, k_3 increases resulting in a further reduction of peroxide to water.

The oxygen electrode is highly irreversible in aqueous electrolyte and this result the substantial energy losses. As it is clear from above that the oxygen reduction takes place at high positive potential (1.23 V vs. SHE) in acid medium. At such a high potential most of the metals will dissolve and only noble metals and their alloys are stable. Among the noble metals, Pt and Pd metals and their alloys appear to be the best electrocatalysts for electrochemical reduction of oxygen [21, 35, 37-39].

1.1.1 Pt and Pt based alloys/ composites

1.1.1.1 Preparation

The ORR activity of Pt-based catalysts depends on particle size, shape and composition, which are strongly affected by the methodology and experimental conditions (e.g., temperature, precursors, pH, etc.) employed in the catalyst preparation. Several methods have been used to prepared Pt-based catalysts, however, only methods, which have been used repeatedly, are briefly described under the following heads.

1.1.1.1.1 Impregnation method

The impregnation method is a simple and the most widely used straightforward chemical preparation technique. In this method, Pt and metal salt precursors are mixed with a high-surface-area carbon powders in aqueous or organic solution (toluene, ethanol, octyl ether, benzyl ether, acetone) to form a homogeneous mixture followed by heating above 700^{o}C under an inert gas (e.g., hydrogen) [40-45]. Alternatively, the mixture is reduced by a chemical reduction in presence of a suitable reducing agent, such as $NaBH_4$ [46], ethylene glycol [47], 1,2-hexadecanediol, formic acid [48-49], formaldehyde [50] borane-tert-butylamine [51-52], etc. Metal chloride and acetate salts are commonly used as precursors in the impregnation–reduction process due to their easy availability.

The heat treatment normally produces a non-uniform composition, resulting in a decrease in the mass activity with the operation time. So, the chemical reduction method is preferentially used for the reduction of metal ions in liquid phase.

1.1.1.1.2 Colloidal method

The colloidal method is another extensively used preparation route for the Pt–based catalysts. This method consists of three steps: preparation of the Pt–metal colloids, deposition of the colloids onto the carbon support and chemical reduction of the suspension [53-55]. The colloidal method can be further optimized by using new precursors, reducing agents, stabilizers, solvents, and synthetic procedures [53-55]. In particular sulfite-complex route, an appropriate amount of $Na_6Pt(SO_3)_4$ is added to the slurry of carbon powders in distilled water, followed by addition of H_2O_2, and its subsequent treatment under a stream of H_2/He as reducing medium [54, 56].

The impregnation method usually produces NPs with large average particle sizes and broad size distributions while the colloidal route produces well-homogenized ultrafine Pt electrocatalysts, however, the complexity of the latter hinders its utilization.

1.1.1.1.3 Micro-emulsion

The emulsion medium consists of an oil-phase (e.g., cyclohexane), a surfactant (e.g., sodium dioctyl sulfosuccinate) and water as an aqueous phase wherein the polar groups of the surfactant are

concentrated in the interior, and lipophilic groups extend outwards into the nonpolar solvent (N-heptane) [57, 58]. In this method, the first step is the formation of Pt–based NPs through a water-in-oil microemulsion reaction, followed by a reduction step. The reduction step can be carried out either by adding a reducing agent (e.g., N_2H_4, HCHO or $NaBH_4$)[46, 57, 58] into the microemulsion system, or by mixing it with another reducing agent-containing microemulsion system. As a result, the reduction reaction is confined to the inside of the nano-scaled microemulsion, and the metal particle sizes, thus formed, can be easily controlled by the magnitude of the microemulsion size. The removal of surfactant molecules can be easily carried out by the heat-treatment of the high-surface-area carbon-supported nanoparticles (NPs). Carbon-supported Pt catalysts with a variety of particle sizes have already been synthesized by the micro-emulsion method [57].

1.1.1.1.4 Seed-mediated growth method

This is one of the most reliable and versatile methods to control the shape of noble metal nanocrystals. The method can be addressed with the preparation of the AuPt/C catalyst [22]. Briefly, Au NPs seeds were obtained by reduction of $HAuCl_4.4H_2O$ with $NaBH_4$ in the presence of trisodium citrate dehydrate as a surfactant. Thereafter, the Pt-precursor salt was added to Au seeds colloidal solution followed by addition of a weak reducing agent like ascorbic acid.

1.1.1.1.5 Core-shell

Recently, a novel class of carbon-supported Pt@PtCu alloy “core-shell” NPs with Pt-Cu alloy core and Pt shell has been developed by selective voltammetric dealloying of Cu from Pt-Cu alloys [59]. The dealloying of Cu from the carbon-supported Pt-Cu alloy electrocatalyst is carried out by subjecting the Pt-Cu alloy to the repeated potential cycling to dissolve less noble Cu from the catalyst surface. The dissolution of Cu from Pt-Cu alloy at high potentials leads to a “core-shell” structured catalyst consisting of a Pt-Cu alloy core encapsulated by a Pt shell. Alternatively, the Pt@Pt-Cu alloy core-shell electrocatalyst (Figure 2) can be obtained after treatment with acid (9 M H_2SO_4).

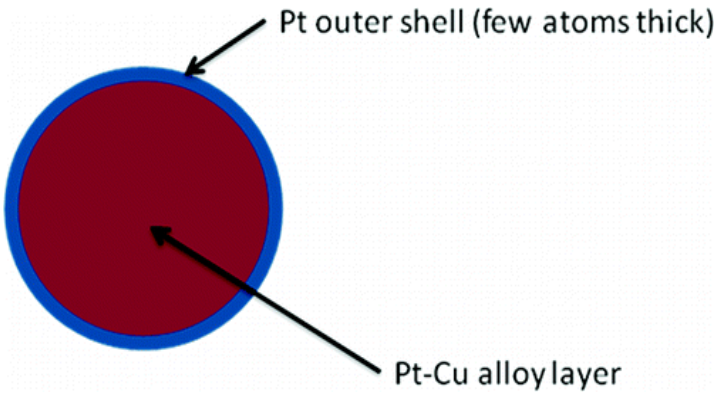

Figure 2. Structural model of Pt@Cu electrocatalysts after treatment with 9 M H_2SO_4. (Reprinted from ref. 59 with permission from American Chemical Society).

Similarly, PtAg alloy NPs rich in Pt at the surface have been obtained through selective electrochemical removal of Ag atoms under different potentials. The size-reduced PtAg alloy NPs with surface rich in Pt were generated when potential was cycled between 0 and 1.2 V (Figure 3) [60].

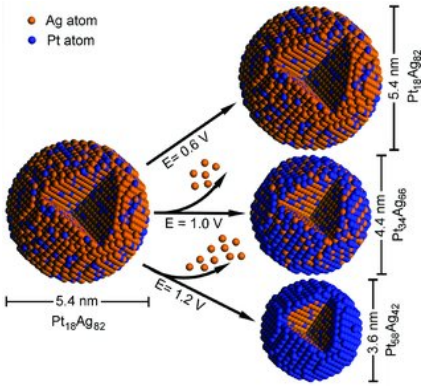

Figure 3. Schematic illustration of compositional and structural changes of the PtAg alloy NPs made by controlled dissolution of Ag metal. (Reprinted from ref. 60 with permission from Wiley-VCH publication).

In CuCoPt ternary particles, Cu was preferably removed from the CuCoPt particles after potential cycles to form the nanostructures having Pt and Co enriched surfaces and compressed surface strain, which enhanced the ORR activity [61].

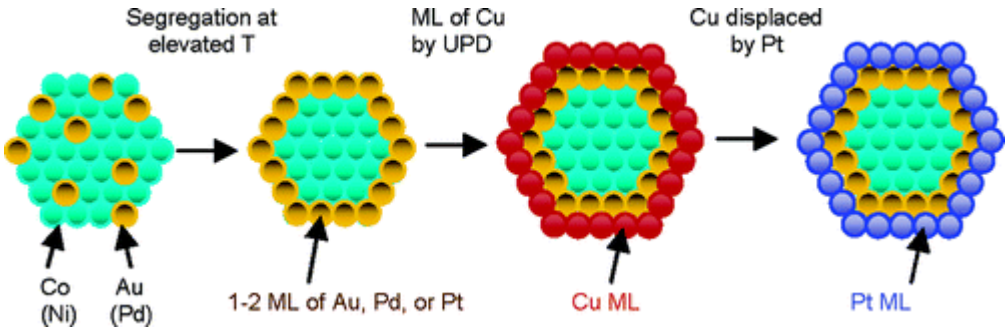

Figure 4. Model for the synthesis of Pt monolayer catalysts on nonnoble metal−noble metal core−shell nanoparticles. (Reprinted from ref. 66 with permission from American Chemical Society).

Another novel class of "core-shell" electrocatalysts, is obtained by Cu underpotential deposition (UDP) on noble metals (Pt, Pd or Au) and subsequent galvanic replacement of the Cu atoms by Pt^{4+} ions. This method produces a single layer of Pt atoms on other noble metal surfaces such as Pd, Ru, and Au. This method is based on the difference in the redox potentials between the metal pairs. In this, Cu (or Ag) is often used as the sacrificial layer and is deposited on noble metals. [62-67].The nonnoble metal-noble metal core-shell NPs were synthesized by segregating the atoms of the noble metal to the NP surface at elevated temperatures [66]. A Pt monolayer was deposited on carbon

supported core-shell metal NPs by the galvanic displacement by Pt of a Cu monolayer obtained by underpotential deposition (Figure 4). The noble metal shell in the core-shell NP protects the non-noble core from contacting the acid electrolyte and improves the catalytic properties of a Pt monolayer by affecting it electronic properties and/or by including strain in a Pt monolayer that increases its activity.

Sarkar and Manthiram [59] synthesized a series of carbon-supported Pt@Cu "core-shell" NPs with a Cu or Pt-Cu alloy core and Pt shell by the galvanic displacement reaction between Pt^{4+} and Cu. Sasaki et al. [68] synthesized Pd@Pt NPs by the Cu-mediated galvanic displacement method, in which a Pt shell was deposited epitaxially onto the surface of a Pd core through galvanic replacement of a pre-deposited Cu layer on a Pd NP seed by Pt precursors.

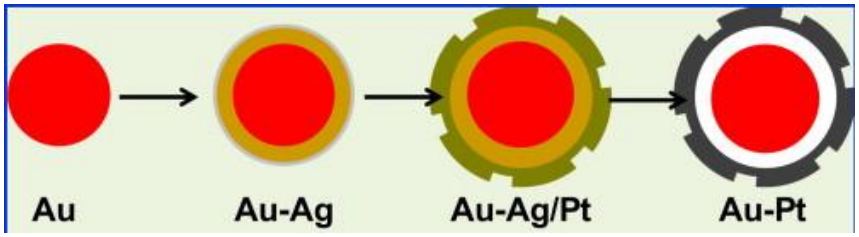

Figure 5. Scheme for preparation of cage-bell structured Au-Pt nanomaterials. (Reprinted from ref. 69 by the permission from Elsevier).

Qu et al. [69] synthesized Au-Pt nanomaterials with cage-bell structures by a template-based approach. For the purpose, Au NPs with narrow size distribution are prepared first, followed by the Ag coating. Then Pt(II) ions are reduced using citrate in presence of core-shell Au-Ag NPs, resulting in the formation of core-shell-shell Au-Ag-Pt NPs with discontinuous Pt shell. Finally, Ag is removed using bis(p-sulfonatophenyl)phenyl phosphane, leaving behind the hydrosol containing the Au-Pt nanomaterials with cage-bell structures (Figure 5). The cage-bell structured Au-Pt nanomaterials displayed superior catalytic activity toward ORR in PEMFCs.

1.1.1.1.6 Hollow Spheres

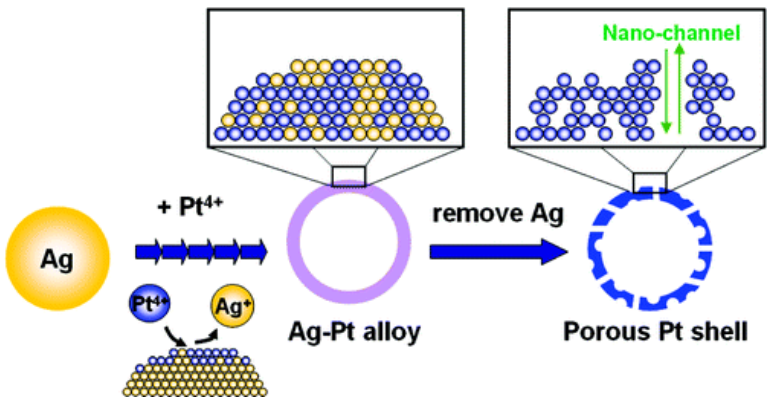

Figure 6. Synthetic Routes of Porous Hollow Pt Nanospheres with Ag Cores and Ag\-Pt Hollow Nanospheres. (Reprinted from ref.23 with permission from American Chemical Society).

The hollow Pt spheres synthesized by galvanic displacement of Ag by Pt^{4+} have been found to offer enhanced activity for the ORR [23]. Figure 6 demonstrates the protocol used to synthesize porous Pt hollow spheres. First of all, the uniform silver nanospheres were synthesized. The second step involved the galvanic replacement reaction between Ag NPs and aqueous H_2PtCl_6 solution ($4Ag + PtCl_6^{2-} \rightarrow Pt + 4AgCl + 2Cl^-$) at room temperature. Pure silver was transformed into a shell of Ag-Pt alloy by galvanic replacement.

1.1.1.1.7 Organic solution approach

In recent years, organic solution approach has emerged as a powerful technique for making monodisperse and homogeneous alloy nanomaterials. Wang et al. [70] prepared Pt_3Co NPs by reducing $Pt(acac)_2$ with 1,2-tetradecanediol (a reducing agent) in the presence of 1-adamantanecaboxylic acid and a large excess of oleylamine followed by $Co_2(CO)_8$ addition and subsequent thermal decomposition.

Very recently, Carpenter et al. [71] prepared Pt-Ni NPs by solvothermal method without use of capping agents in which DMF functions as both solvent and reducing agent. Jackson et al. [72] prepared Ru@Pt core-cell NPs using a liquid-phase synthesis. Briefly, ruthenium acetylacetonate is reduced in refluxing ethylene glycol with polyvinylpyrrolidone to form Ru NPs which serve as core. After cooling, chloroplatanic acid is added to the solution, which is then slowly heated to form the Pt shell. Gan et al. [73] synthesized Pt_xNi_{1-x} core-cell NPs by a modified low temperature organic solution approach where Pt $(acac)_2$ and $Ni(acac)_2$ acted as precursors, oleylamine and oleic acid as surfactants and 1,2 tetradecadiol as the reducing agent.

1.1.2 Research work on ORR

Pt is the most efficient and extensively studied electrocatalyst for ORR because it exhibits good activity and stability under the operating conditions. But, Pt is costly metal and so, to reduce the cost and enhance the efficiency, Pt is, generally, obtained in highly dispersed form on different high surface area carbon supports. Among all kinds of carbon supports, namely activated carbon, carbon black, graphite, and graphitized materials, carbon black is the most commonly employed and investigated for fuel cell electrocatalysis. It is due to fact that carbon black has low cost, good electronic conductivity, chemical and mechanical stability, high surface area and appropriate pore structure [74]. The graphitic carbon exhibits higher resistance to corrosion than the non graphitic carbon one [75]. Carbon supports are obtained by burning carbonaceous materials and so, their properties strongly depend upon the nature of the starting materials and the preparation conditions, such as activation method, temperature and heating time [76]. It is known [77] that the surface of the carbon support has some oxygen functional groups, such as carbonyl (C=O), carboxylic (-COOH), phenolic (Ph-OH), anhydride ($(R-CO)_2-O$), lactonic (-C(CO)OC-) and etheric (R-O-R') groups. The surface oxygen-based groups can act as active or anchoring centres for generation of highly dispersed metallic crystallites. Therefore,

electrocatalyst loading and dispersion and performance significantly depend upon the nature of functional groups present on the catalyst surface [78-79].

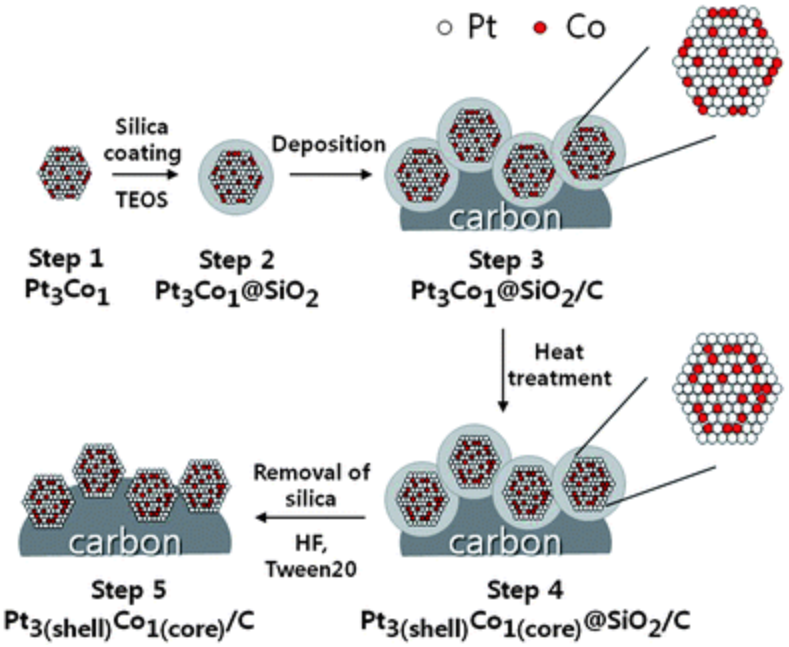

Figure 7. Schematic illustration of the synthesis of the Pt_3Co_1/C catalyst using the silica encapsulation process: (1) preparation of PVP-stabilized Pt_3Co_1 NPs; (2) formation of the SiO_2 coating; (3) deposition onto the carbon support; (4) calcination; (5) removal of SiO_2 coating using HF in the presence of Tween 20. (Reprinted from ref. 80 by the permission from Royal Society of Chemistry).

The activity for ORR and tolerance for MOR of Pt catalysts can be increased by mixing other metals such as Cr, Fe, Co, Ni, Cu, Bi, Sn and Au etc.[20]. The heat treatment strongly influences the ORR activity and stability of fuel cell catalysts. In case of Pt-based catalysts, the heat treatment can induce particle-size growth, better alloying degree, and changes in the catalyst surface morphology from amorphous to more ordered states, which have remarkable effect on the ORR activity and stability. The major effects of heat treatment on catalyst properties, including particle size, morphology, dispersion of the metal on the support, alloying degree, active site formation, catalytic activity, and catalytic stability are comprehensively reviewed [74]. As the heat treatment of the alloy NPs generally results in severe sintering, the heat treatment of the catalyst at a too high temperature (>1000 ^{0}C) is, therefore, not recommended. To prevent sintering during the heat treatment at a high temperature in the case of carbon-supported Pt_3Co_1 alloy NPs, Oh et al. [80] recently reported a new synthetic process of silica encapsulation (Figure 7). The silica layer acts as a physical barrier to prevent sintering and thereby the carbon-supported Pt_3Co alloy NPs retained their small particle size. During the heat treatment, atoms rearrange themselves producing the alloy NPs surface rich in Pt. Consequently, the catalytic activity and stability of the carbon-supported Pt_3Co alloy NPs get improved considerably.

Antolini et al., [81] demonstrated that among Pt-Cr (Pt:Cr = 9:1, 3:1 & 1:1) alloys on C, the Pt_9Cr/C catalyst exhibited the highest ORR and the lowest MOR activity. The decrease in MOR activity has been attributed to "ensemble effect" which is, in fact, the dilution of the active component with catalytically inert metal by alloying, resulting in re-distribution of active sites [82]. In fact, the dissociative chemisorption of methanol requires the existence of several (at least three) adjacent Pt ensembles [5, 83] and so, the presence of second metal blocks the methanol adsorption on Pt sites and thereby suppresses the methanol oxidation. On the other hand, the oxygen adsorption, which requires only two adjacent sites, is not affected by the presence of second metal (M). To avoid an undesired metal particle growth by Pt and M alloying, the carbon supported oxygen reduction catalysts are generally prepared at low temperatures (<700°C) [76-79, 84]. Similar Pt-Cr/C alloys (Pt:Cr = 3:1, 2:1 and 1:1) catalysts, prepared through carbonyl chemical route, observed a slight enhancement in the mass activity (MA) and a significant enhancement in the ORR specific activity (SA), by a factor of 1.5-3 in the absence of methanol [85, 86]. Moreover, a significant enhancement in both the SA and MA was observed in the presence of methanol as compared to Pt/C catalyst. The activities of non alloyed Pt-Cr catalysts were lower than the alloyed catalysts but better than Pt [87]. This may be caused due to higher electronic interaction between Pt and Cr, the change of Pt-Pt lattice parameter and greater Pt coverage by Cr in the alloyed catalysts than non-alloyed ones, which reduces the accessibility of oxygen to the Pt active sites.

Shukla et al. [88] observed high ORR activity on the Pt-Fe/C alloy in 0.5M H_2SO_4 in presence of methanol while Pt/C suffers from the methanol poisoning effect. The methanol crossover causes a little change in the active catalyst area for Pt-Fe/C during the fuel cell operation [89]. Yuan et al. [90] also found an increase in power density up to 20-30% on the Pt-Fe alloy electrocatalyst (Pt:Fe=1:2.7, 1.2:1, 3.8:1) than that on Pt/C, prepared by the impregnation method. It was observed by Scott et al. [91] that Pt-Fe/C (Pt : Fe = 3.8:1, 1.2:1, 1:2.7) alloy catalysts prepared by the impregnation method show higher ORR activity and stability compared to Pt/C in methanol containing and methanol free electrolyte and they are better methanol tolerant also. Better methanol tolerance of the PtFe alloy is because of the fact that Fe itself is not active for MOR and its addition will partly block contact between Pt-particle and methanol molecules, reducing the adsorption of methanol. Also, based on quantum calculations, the strong reactivity of Pt with organic component is depressed by alloying with Fe, resulting in high methanol tolerance [92]. Chen et al. [93] investigated the ORR study on Fe_xPt_{100-x} NPs (x = 63, 58, 54, 42, 15, and 0)/ GC electrodes in 0.1 M $HClO_4$, the ORR activity being maximum with $Fe_{42}Pt_{48}$/GC. The ORR followed the four-electron transfer mechanism in 0.1 M $HClO_4$.

Xiong and Manthiram [94] synthesized nanostructured Pt-M/C (M = Fe and Co) by a micro-emulsion method and a high temperature route. They observed higher ORR activities with the catalysts in a proton exchange membrane fuel cell (PEMFC). The Pt-Co/C electrode exhibited the best performance. Further, the heat treatment of the catalysts at a moderate temperature (200 ºC) in reducing atmosphere improved the catalytic activity due to cleaning of the surface and increase in the electrochemical surface area. Lima et al. [95] investigated the ORR on carbon-supported composites of Pt and a metal (V, Cr, Or Co) in 1:1 nominal atomic ratios and 20 wt% metal/C in 1 M KOH. Results indicated a higher catalytic activity for Pt-V/C. This was attributed to a lowering of the adsorption

strength of adsorbed oxygen species caused by the increase of the Pt 5d occupancy, promoted by the V atoms in the Pt lattice.

Salgado et al. [96] investigated the ORR on carbon supported Pt and Pt-Co alloys (Pt:Co = 85:15, 75:25) in presence and absence of methanol in 0.5 M H_2SO_4 and in DMFC and obtained enhanced ORR activity and methanol tolerance with the alloy electrocatalyst. The high methanol tolerance is ascribed to the low activity of the binary electrocatalyst for MOR. Contrary to this, Siracusano et al. [97] reported the Pt-Co/C (Pt:Co = 3:1) electrode, prepared by a colloidal method, as less tolerant to MOR. This has been attributed to the enhanced metallic character of Pt in the Pt_3Co due to intra-alloy electron transfer from Co to Pt and to the adsorption of CO on the more electropositive element (Co) that promotes MOR according to the bifunctional theory. Wang et al. [98] synthesized monodisperse Pt_3Co NPs with size control via an organic solvothermal approach. NPs, so obtained, were incorporated into a carbon matrix and investigated as electrocatalysts for the ORR. The optimal conditions for maximum mass activity were with particles of ~ 4.5 nm and a mild annealing temperature of about 500 ºC [99].

Hwang et al [100] investigated the structure-catalytic activity relationship for Pt-Co/C bimetallic NPs toward the ORR. Alloys were prepared via a modified Watanabe process by employing microwave heating. As compared to the Pt/C catalyst, the bimetallic Pt-Co/C catalysts exhibited an enhancement factor of 3 in the mass activity at 0.95 V toward ORR. The activity enhancement might originate from the favourable electronic effects of a well mixed alloy underneath a thin "Pt-rich skin" structure of the Pt-Co bimetallic NPs. This "Pt-rich skin" is created by the dissolution of Co-oxide from the Pd-Co alloy surface while washing in acidic electrolyte before being subjected to the ORR study. Dsoke et al. [101] studied the ORR on novel types of carbon-supported Pt-Co alloys and Pt-Co-$Cs_{2.5}H_{0.5}PW_{12}O_{14}$ composite electrodes by RDE (rotating disc electrode) voltammetry in O_2-saturated acidic medium. The composite electrodes showed better performances towards ORR than the commercial pristine catalyst in terms of mass activities, the activity being higher with Pt-Co alloy. Okaya et al. [102] prepared new cathode catalysts comprising of two monolayers of Pt deposited on PtCo alloy particles of fcc solid solution-supported on graphitized carbon black (GCB) (cathode: Pt_{2ML}-PtCo/GCB) by a modified nanocapsule method. Very recently, Yang et al. [103] observed that the kinetics of the ORR in acid solutions greatly depends upon the number of Pt monolayers on Ru@Pt core shell NPs, and the optimum activity occurs with two Pt monolayers.

Similarly, carbon-supported Pt-Ni alloys were prepared with varying Ni contents using the carbonyl chemical route [104]; these electrodes were highly methanol tolerant and their specific activities towards the ORR followed the order: Pt-Ni(2:1)/C > Pt-Ni(1:1)/C > Pt-/C. In the single cell test the maximum power density with Pt:Ni (2:1) was 101.5 mW cm^{-2} as compared to 80.3 mW cm^{-2} for a Pt/C catalyst. The low reactivity of Pt-Ni toward MOR during the ORR has been ascribed to the composition and the ensemble effects. Drillet et al. [105] also observed a significantly enhanced activity for ORR at a PtNi alloy, the ORR being, however, shifted to more positive electrode potentials in the methanol containing electrolyte.The mass transport corrected Tafel slopes were 83 mV for PtNi and 120 mV for Pt. Pt-Ni/C (Pt:Ni = 90:10, 70:30) electrodes synthesized by sodium borohydride reduction method [106] contained about the same amount of alloyed Ni (6-8 at%) but different amounts of non-alloyed Ni. Pt-Ni/C showed better performance than Pt both in terms of MA and SA.

The enhanced methanol tolerance was ascribed to the alloyed Ni and that the presence of non-alloyed Ni or NiO does not affect the performance of DMFC. In the methanol free electrolyte (H_2SO_4), $Pt_{70}Ni_{30}$/C displayed lower SA than Pt for ORR but higher activity in methanol containing electrolyte. The high ORR activity may be ascribed to the low activity of the binary electrocatalyst for MOR arising from the composition effect [107]. Pt-Ni alloy NPs supported on carbon black (Pt:Ni = 1:1) were also obtained by the borohydride reduction method using acetate anions as a stabilizer in anhydrous ethanol solvent [108]. Though as-prepared Pt_1Ni_1/C exhibited a relatively high degree of alloying, it showed the lower ORR activity as compared to pure Pt. Pt-Ni alloy catalyst showed the higher ORR activity than that of commercial Pt/C (40wt% Pt/C, Johnson – Matthey) when heat treated in a flow of Ar at 300ºC for 3 h. The observed increase in the ORR activity by heat treatment is due to increase of metallic Pt and Ni oxides.

Seo et al. [109] prepared ternary alloys of Pt with Co, Cu, Cr, and Ni by incipient wetness method [110]. In the unit cell test, these ternary alloys showed higher ORR activities compared to Pt/C, the performance being the best with $Pt_6Co_1Cr_1$. Carbon-supported ternary PtVFe electrocatalysts, obtained by thermal decomposition and reduction reactions also exhibited higher ORR activities in 0.5M H_2SO_4 [111]. The ORR activities of Pt-Co-Mn ternary electrocatalysts deposited on NSTF (nano-structured thin film) in 0.1M $HClO_4$ were also higher than Pt/NSTF [112]. Electrocatalysts were deposited on NSTF support using a multi-target sputtering system. A two-fold kinetic gain for Pt-Co-Mn/NSTF over Pt/NSTF was observed.

Maillard et al. [113] reported that the enhancement in methanol tolerance and ORR activity of Pt based catalysts is a function of decrease in the particle size. Similar results were also observed by Stassi et al. [56] in the ORR study on 60 wt% Pt-Fe/C and Pt-Cu/C catalysts, prepared by using a combination of colloidal and incipient wetness methods. The performances of Pt-Cu/C and Pt/C were similar while it was superior with Pt-Fe/C and that the activity increased by increasing the temperature. According to the authors, the smaller particle size of Pt-Fe/C (2.4 nm) with respect to Pt/C (2.8 nm) is responsible for the enhanced activity. Baglio et al., [114] also observed superior catalytic activity and methanol tolerance for Pt-Fe/C compared to Pt/C, Pt-Co/C and Pt-Cu/C catalysts in the single cell DMFC at 60°C. The enhanced catalytic activity of PtFe catalyst has been attributed to the presence of a Pt skin over the alloy together with an electronic effect induced by Fe on Pt [115]. The improvement in the performance may also be partly due to higher peroxide decomposition on Pt in presence of dissolved Fe favouring the $4e^-$ transfer route [116].

Recently, Nesselberger et al. [117] examined the influence of particle size on the ORR activity of Pt in three different electrolytes: $HClO_4$, H_2SO_4 and KOH. The activity trend for the ORR with increasing particle size is independent of the electrolyte and it rapidly decreases going from polycrystalline Pt, to unsupported Pt black particles and high surface area (HSA) carbon supported Pt NPs. Shao et al. [118] determined the specific and mass activities of the ORR in $HClO_4$ solutions on the Pt particles in the range of 1 – 5 nm. The mass activity increases by 2-fold from 1.3 to 2.2 nm. On the other hand, the specific activity increases rapidly by 4-fold as the particle grows to 2.2 nm and then slowly as particle size further increases.

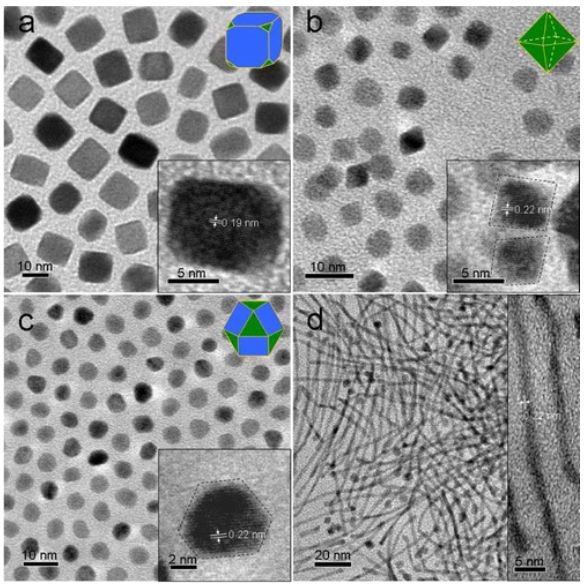

Figure 8. The TEM and HRTEM image of PtNiFe nanostructures, including (a) nanocubes, (b) octahedrons, (c) polyhedrons, and (d) nanowires. The graphic representation shows the three-dimensional image of nanocubes, octahedrons, and polyhedrons. Blue and green represent the {100} and {111} facets, respectively. (Reprinted from ref. 121 with the permission from American Chemical Society).

In the ORR study on Pt_3Ni, Zhang et al. [119] observed that the activity of the catalyst depends upon the shape of the catalyst particle. They prepared nano-octahedral and nano-cubes (NCs) through wet chemical method with (111) and (100) facets, respectively, and found that (111) facet terminated octahedral are more active than (100) bound nanocubes; the ORR activity being ~5 fold. The ORR activity of the Pt_3Ni octahedral is further improved by the decrease in the size. Wu et al. [120] also reported that the activity is dependent on the shape and composition. They prepared truncated octahedral Pt_3Ni with (111) facet and obtained ~4 times higher mass activity than Pt/C and 1.8 times higher than octahedral Pt_3Ni/C. Chou et al. [121] synthesized PtNiFe nanostructures with the various shapes of nanocube, polyhedron, octahedron, and nanowire successfully through the fine adjustments of crystal facet-surfactant bindings (Figure 8). The latter can be adjusted via fine tuning of the alloy composition and surfactant. The study of ORR electrocatalysis indicated that the ORR activities of all PtNiFe nanostructures outperform to that of commercial Pt catalyst in $HClO_4$ or H_2SO_4. Carpenter et al. [71] also obtained well-faceted cubic and octahedral nanocrystals of Pt_3Ni, and octahedral and truncated octahedral nanocrystals of PtNi through the solvothermal method using DMF as both solvent and reductant. These Pt alloy nanocrystals were found to have ORR specific activities 3-5 times greater than that of a Pt standard catalyst.

Meng and Shen [122] prepared tungsten carbide nanocrystals and tungsten carbide nanocrystals-modified Pt catalysts by an intermittent microwave heating (IMH) method and tested for the ORR in alkaline media for the first time. The results revealed that both of them were active for the ORR in alkaline media. The overpotential was significantly reduced on the tungsten carbide nanocrystal-modified Pt catalyst, showing a synergetic effect to improve the activity for ORR. Similar catalysts on carbon support (Pt-W_2C/C) had 100 mV more positive onset potential compared to that of

traditional Pt/C electrode in acidic media [123]. The novel electrocatalysts displayed a poisoning resistant property toward MOR. Travitsky et al. [124] observed that SiO_2-supported Pt and Pt alloy powders had larger grains and lower EASAs than the carbon-supported catalysts. This is attributed to the strong interaction of the metal particles with the silica support, resulting in an enhanced agglomeration of their surface. Alloying Pt with Co and with Ni led to ~40 and 50% reduction, respectively, in the grain size of both catalyst types. The EASAs of carbon-supported catalysts increased by 100% and 200% by alloying respectively with Co and Ni. The alloy catalysts were highly stable in acid medium. Also, catalysts post-treated in acid were stable and had a Pt-rich (or pure) "skin" structure. Pt supported on nano-tungsten carbide is a beneficial catalyst for the ORR [125]. Elezovic et al. [126] synthesized Pt nanocatalysts on two tungsten based supports, WCctabar (80 m^2g^{-1}) and WC_{WO3} (175 m^2g^{-1}) by borohydride reduction method in 0.5 M $HClO_4$ exhibited better catalytic activity and better stability in comparison with Pt/C catalyst as well as with already reported catalytic activity values for Pt catalysts on tungsten based supports.

Pt/W_xC (x =1 or 2) hybrid nano-catalyst supported on carbon black (CB) were synthesized using a simple co-impregnation and thermal reduction method. 5 wt% Pt-doped W_xC catalyst shows significant enhancement in ORR performance in alkaline medium which is comparable to that of the 20wt% Pt/C catalyst. The synergetic effect of Pt/W_xC which arises from the charge transfer of metal-metal hybrid interaction are the cause of the enhancement. [127]. Garcia et al. [48] also observed an enhancement in the ORR activity compared to Pt/C with Pt catalyst dispersed on tungsten carbide(WC) prepared with a high surface area carbon with two different WC/C ratios in alkaline electrolyte. The ORR involves a transfer of 4 electron per oxygen molecule.

Xu et al [128] employed a one-pot thermal decomposition method to prepare three-dimensional platinum nanochain network (Pt-3NCNW) nanostructures in the absence of any surfactants and templates for application in PEMFCs. Compared to the commercial Pt black catalyst, the Pt-3NCNW nanostructures exhibited superior electrocatalytic activity and stability toward ORR (Electrolyte: O_2-saturated 0.5 M H_2SO_4). The improved activity of Pt-3NCNW was attributed to the few surface defect sites, the numerous low energy crystal facets, the low hydroxyl surface coverage on 1D Pt nanochains, as well as fast O_2 diffusion in 3D structures.

Yano et al [129] succeeded to obtain Pt and Pt-M (M = V, Cr, Fe, Co, and Ni) alloy NPs in highly dispersed form on CB support by the simultaneous reduction of $Pt(acac)_2$ and $M(acac)_x$ in organic nano-capsule. It was observed that the ORR activity at the Pt-V/CB, Pt-Cr/CB, Pt-Fe/CB, Pt-Co/CB and Pt-Ni/CB were higher than that of Pt/CB catalyst. This method of synthesis has good control of both the particle size (mono dispersion) and uniform alloy composition.

Using reverse Micelle method, Qian et al [58] prepared PtM/C (M = Co, Cr, or Fe). The PtM/C catalysts in 1 M $HClO_4$ followed the ORR activity order: PtCo/C(T, 500) ~PtCo/C(S) > PtCr/C(S) > PtFe/C(S) ~ Pt/C > PtFe/C(T, 500), showing that PtCo/C-type catalysts had a higher catalytic activity for ORR. The number of exchanged electron in the ORR was found to increase from 3.4 to 4.2 when the sintering temperature increased from 200 to 500 ºC.

Gupta et al. [130] designed and synthesized highly stable and highly active Pt-Cu NPs catalyst on graphitized mesoporous carbon (MC) with a pre-synthesis/infusion technique. The unprecedented

stability of these highly graphitic bimetallic ORR catalysts and a negligible loss in EASA as well as catalytic activity (<2% for both) after 1000 cycles between 0.5 V and 1.2 V have been claimed.

Carbon-supported Pt and Pt-M (Fe, Co and Cr) alloy catalysts prepared by simultaneous Polyol reduction and decomposition of metal precursors with 1,2 hexadecanediol in presence of nonanoic acid and nonylamine protecting agents produced spherically shaped NPs with a narrow size distribution [131]. Pt alloys exhibited ~1.5 times higher ORR activity and ~ 50 mV lower overpotential than that of Pt/C catalysts. The enhancement of ORR activity is ascribed to the inhibition of formation of (hydr) oxy species on the Pt surface by the presence of alloying elements. Single cell DMFC tests also showed the good performance of Pt alloys compared with that of the Pt/C catalysts. On the other hand, Pt- and Au-coated Fe, Co, Ni, and Pb particles deposited on GC electrode in acid solutions exhibited a decrease in ORR activity with Pt(Fe)/GC, Pt(Co)/GC and Pt(Ni)/GC electrodes, in accordance with a strong electronic effect of the M-containing core to the Pt shell. Similar effect was also observed in the case of Au or Pt(M)/GC (M = Fe, Co, Ni or Pb) electrodes [132]. Fe, Co, Ni or Pb layers were electrodeposited onto GC and subsequently immersed into chloroplatinic acid or chloroauric acid solutions where the spontaneous surface exchange of M for Pt or Au resulted in Pt(M)/GC and Au(M)/GC electrodes. Fe, Co, and Ni down-shift considerably Pt e_d and hence weaken significantly its affinity for oxygenated species, thus shifting Pt from the top of the corresponding volcano plot towards the Ag, Au, etc. branch of the plot. On the contrary, Pt(Pb) deposit showed a slight increase in Pt catalytic activity. All Au(M)/GC electrodes exhibited an increase in ORR activity in acid. The enhancement may be due to increased electrochemical desorption of intermediates.

Zhang [133] demonstrated that platinum oxygen reduction fuel cell electrocatalysts can be stabilized against dissolution under potential cycling regimes by modifying Pt NPs with gold clusters. Insignificant changes in the ORR activity and surface area of Au-modified Pt electrocatalysts were observed under potential cycling between 0.6 and 1.1 V in over 30,000 cycles. They also prepared [134] a new class of electrocatalysts, consisting of Pt and another late transition metal (M, where M = Ir, Ru, Rh, Pd, Au, Re, or Os) deposited as a monolayer on the surfaces of Pd(111) single crystal or carbon-supported Pd NPs, that can greatly improve the ORR activity and reduce the mass of the Pt. These new electrocatalysts have very high activity compared to that of pure Pt ORR catalysts and a considerably lower Pt content. A gain in current density up to a factor of 400% compared to all-Pt has been realized by replacing part of the Pd-supported Pt monolayer with another transition metal, M, where M = Ir, Ru, Re, or Os. The very high catalytic activity measured for the Pd-supported Pt-M mixed monolayer, with M adsorbing OH or O strongly, reflects the decreased OH coverage on Pt, caused by the lateral repulsion between the OH adsorbed on Pt and the OH or O adsorbed on a neighbouring surface metal atom, M. Hence, the role of the second metal is to lower the OH coverage on Pt. They also synthesized Pt [66] monolayers deposited on the surfaces of carbon-supported non-noble metal-noble metal core-shell NPs (Figure 4). The mass activity of all the three Pt monolayer electrocatalysts, namely Pt/Au/Ni, Pt/Pd/Co and Pt/Pt/Co, investigated, was more than order of magnitude higher than that of a state-of-the-art commercial Pt/C electrocatalyst. These new class of catalysts have a high activity and very low noble metal content. In similar studies carried out by Vukmirovic et al. [135], several of these electrocatalysts exhibited very high activity, amounting to 20-fold increase in a Pt mass activity, compared with conventional all-Pt electrocatalysts.

Nilekar et al.[136] synthesized and tested a new class of electrocatalysts for the ORR that were based on monolayers of Pt deposited on different late transition metals (Au, Pd, Ir, Rh, or Ru), of which the Pd-supported Pt monolayers had the highest ORR activity. The amount of Pt used was further decreased by replacing part of the monolayer with a third late transition metal (Au, Pd, Ir, Rh, Ru, Re, or Os). Several of these mixed Pt monolayers deposited on Pd single crystal or on carbon-supported Pd NPs exhibited up to a 20-fold increase in the ORR activity on a Pt-mass basis when compared with conventional all-Pt electrocatalysts. From DFT calculations, it is demonstrated that their superior activity originated from interaction between the Pt monolayer and the Pd substrate and from a reduced OH coverage on Pt sites, the result of enhanced destabilization of Pt-OH induced by the oxygenated third metal.

The Pt/Au/C catalyst prepared by depositing Pt and Au NPs on carbon support showed enhanced methanol tolerance [137] as well as ORR activity [138] than Pt/C. The high methanol tolerance could be ascribed to ensemble effect as previously reported [81] and to the unique surface structure of the Pt/Au/C catalyst. According to the DFT calculations, there occurs an intra alloy electron transfer from Pt to Au in Pt-Au alloy which is responsible for the synergistic promotion of the oxygen reduction on the Pt-Au electrode. The DMFC with Pt-Au/C alloy as cathode catalyst showed the peak power density of 120 mW cm^{-2} in relation to 80 mW cm^{-2} for Pt/C cathode. The ORR activities of PtRh/C catalysts in 0.5 M H_2SO_4 were also higher than Pt/C. Of these, PtRh (2:1) alloy cathode showed a higher power density as well as better performance stability in DMFC unit cell test.

Lopes et al. [17] prepared a carbon-supported Pt-Pd catalyst with a Pt:Pd atomic ratio77:23 by reduction of metal precursors with formic acid. A decrease in the lattice parameter compared with that of pure Pt was observed, indicating the formation of a Pt-Pd alloy. The ORR study in H_2SO_4 solution in presence of ethanol showed a large increase in overpotential of the ORR on pure Pt than that on Pt-Pd, indicating a higher ethanol tolerance of the binary catalyst. The results of the direct ethanol fuel cell (DEFC) test with Pt-Pd/C as cathode at 90^0C also confirmed the findings of half cell tests. However, Jeyabharti et al.[139] observed that, in the case of Pt-Sn/C bimetallic NPs, the alloying of Pt with Sn (Pt-Sn/C) and the heat treatment increased the particle size as well as the lattice parameter. They observed ORR activities in the order: Pt-Sn/C (as prepared) > Pt-Sn/C(250°C) > Pt-Sn/C(500°C) > Pt-Sn/C(600°C)/Pt-Sn/C (800°C). The ORR followed first order kinetics with a Tafel slope of 120 mV. Carbon-supported Pt-Fe/C bimetallic nanocatalysts with varying Pt:Fe ratio obtained by a modified ethylene glycol method and subsequent heat treatment under H_2-Ar (10 vol%-H_2) atmosphere at 900^0C indicated [140] that the Pt-Fe/C with a Pt:Fe ratio of 1.2:1 and an optimized lattice parameter of around 3.854 Å has the highest mass activity and specific activity to the ORR. As cathode catalyst, this active electrode exhibited higher DMFC performance at 90^0C than Pt/C and other Pt-Fe/C catalysts. Addition of Fe is found to prevent Pt particles agglomeration effectively. Also, carbon supported Pt-Cu catalyst (Pt-Cu/C) with surface enriched Pt by annealing showed [44] 3.7 times higher Pt mass activity toward the ORR than commercial Pt/C in O_2-saturated 0.5 M $HClO_4$. The enhanced ORR activity of PtCu/C is attributed to the modified electronic properties of surface Pt atoms, which reduces the surface blocking of the ORR oxygenated species. Bimetallic PtAg/C catalyst synthesized by the chemical reduction exhibited the activity comparable to that of commercial Pt/C (from ETEK)

for ORR in 0.3M KOH under O_2 atmosphere and exhibited high selectivity for ORR in the presence of glucose in 0.3M KOH [141].

Sarkar et al. [142] synthesized carbon-supported multimetallic nanostructured alloys of Pt, Pd, and Co with high crystallinity and homogeneity by a one-pot rapid micro-wave assisted solvothermal (MW-ST) method within 15 minutes at <300 ^{0}C without any post-annealing in reducing gas atmospheres. The ORR activities of alloys were much higher compared to their counterparts synthesized by the conventional borohydride reduction method. The ORR activity of $Pt_{70}Pd_{20}Co_{10}$ was comparable to that of commercial Pt while that it was superior due to high tolerance of the ternary composite toward methanol oxidation, particularly at high methanol concentrations. Wang et al. [143] prepared a multi-component novel nanocomposite Cu/PtFe/ carbon nanotubes (CNTs) as a cathode catalyst for DMFCs. The effects of Fe and Cu on ORR activity and methanol tolerance were investigated by varying their amounts. Results showed that PtFe alloy on CNTs could not enhance methanol tolerance, but it improved the ORR activity. Cu was deposited on PtFe/CNTs to obtain better methanol tolerance. The optimum molar ratio of Cu/Pt/Fe/CNTs was observed to be 2.1:1:0.7. After 500 cycles in 1 M $HClO_4$ solution, the Cu/PtFe/CNTs catalyst exhibited fairly stable performance, maintaining 92% of its original ORR activity and 89.6% of its original electrochemical active surface areas (EASA).

Ghosh et al. [144] prepared Pt-Pd alloy nanoparticle-decorated CNTs and investigated as electrocatalysts for the ORR using the RDE method in 0.5 M H_2SO_4. The $Pt_{46}Pd_{54}$ catalyst outperformed the electrocatalytic activity among the series. Further, it was highly durable and it retained its initial catalytic activity even after 1000 extensive cycles. Its ORR activity was also higher than the commercially available Pt black and MWCNT-supported spherical Pt NPs. Pt-Pd alloy nanoelectrocatalysts of different compositions were obtained by the impregnation route using a modified polyol procedure.

Wang et al. [145] synthesized a novel Pt nanosponge foil (Pt-NSF) using Pluronic F127 ($PEO_{100}PPO_{65}PEO_{100}$) as the reducing agent. The electrochemical active areas (EASA) of the Pt-NSF and Pt-black were of the order of 20 m^2g^{-1}. The mass activity and specific activity of Pt-NSF were much higher than each of Pt-black toward the ORR in 0.1 M $HClO_4$. Durability tests showed that the EASA of Pt-NSF and Pt-black declined, but the activity of Pt-NSF toward the ORR was almost unchanged.

In the RDE experiments carried out in 0.5 M H_2SO_4/0.1M KOH solutions, sputer-deposited Pt NPs supported on multiwalled carbon nanotubes (MWCNTs) (PtNP/MWCNT) also indicated a high ORR activity compared to commercial Pt/C catalyst and bulk Pt and the reaction followed a 4-electron pathway [146]. Two Tafel regions with the characteristic slopes close to -60 and -120 mV were found. The nominal film thicknesses were 4, 8 and 16 nm and the corresponding Pt loadings were 8.6, 17.2 and 34.4 μg cm^{-2}, respectively (calculated per geometric area of the GC substrate).

Recent studies on single crystalline thin films have revealed that the addition of an early transition metal (Fe, Co, or Ni) to Pt can change the geometric (Pt-Pt bond distance and coordination number) and electronic structure of Pt [147, 148]. Due to these structural changes, the adsorption of OH is mostly centred on the second metal, not on Pt, and oxygen tends to be reduced on Pt in a "four-electron" process. The ORR catalytic activity of these alloys is also dependent on the type and

concentration of the second metal in the substrate atomic layers. Considering these results, Kim et al. [149] obtained FePt NPs and used in the study of ORR catalysis. The FePt NPs are much better electrocatalysts for ORR and their activities are the structure dependent. Monodisperse FePt NPs with control of Fe, Pt composition have been synthesized [150, 151]. These FePt NPs have the chemically disordered face centred cubic (fcc) structure within which Fe and Pt atoms are positioned randomly in the fcc lattice. Under high temperature annealing conditions, the fcc structure can be converted to a chemically ordered face centred tetragonal (fct) structure with Fe and Pt intermetallically stacked. However, this annealing also leads to serious NP aggregation/sintering. Results indicated that the fcc-FePt NPs are more active and durable than the fcc-FePt NPs for ORR in 0.5 M H_2SO_4 due to its stable intermetallic Fe, Pt arrangement.

Recently, it is observed that the Pt surface modified with nitrogen (PtN_x/C) shows significant methanol tolerance as compared to commercial Pt/C while maintaining their high activity towards ORR [109]. The high methanol tolerance behavior of the catalyst can be attributed to the modification of the surface with nitrogen which prevents methanol from adsorbing on the Pt active sites while oxygen is not perturbed for the reduction reaction. Later, Oh and Kim [152] reported that the heat treatment temperature and the molar ratio of Pt to N play important roles in the activity performance of the catalyst. The heat treatment higher than 500 °C is effective to modify the Pt surface. The ORR activity decreases with an increase in the molar ratio of N. Gao et al. [153] developed a facile and in situ template-free synthesis of Pt containing mesoporous nitrogen-doped carbon composites (Pt-m-N-C). The as-prepared Pt-m-N-C catalyst exhibits high electrocatalytic activity, dominant four-electron oxygen reduction pathway, superior stability, fuel crossover resistance, and selective activity to a commercial Pt/C catalyst in 0.1 M KOH aqueous solution. Banis et al. [154] synthesized composites of $TiSi_2O_x$ coated nitrogen-doped carbon nanotubes (NCNTs) by a combination of chemical vapour deposition (CVD) and magnetron sputtering process and were used as supports for Pt catalyst for ORR in PEMFCs. The $Pt/TiSi_2O_x$-NCNTs catalysts showed better catalytic activity towards ORR than Pt/NCNT catalysts.

To reduce the usage of Pt and improve the reactivity of Pt, Yin et al. [155] have synthesized the vanadium nitride/graphitic carbon (VN/GC) nanocomposites as new Pt support for the first time. After loading only 10% Pt NPs, the resulting Pt-VN/GC catalyst demonstrates a more positive onset potential (1.01 V), higher mass activity (137.2 mA mg^{-1}), and better cyclic stability (99% EASA retention) after 2000 cycles towards ORR than the commercial 20% Pt/C. The ORR follows 4e-transfer mechanism. Inoue et al [156] heat treated Ketjen Black EC300J (Lion Corp.) at different temperatures in the range 1000-2000 ºC under a N_2 stream for 1h using an infrared image furnace and then Pt catalyst was loaded on them by impregnation from a $Pt(NO_2)_2(NH_3)_2$ ethanol solution. A maximum enhancement in the specific ORR activity was observed for the carbon heat treated at 1500 ^{0}C. The electrolyte used was O_2-saturated 0.5 M H_2SO_4.

Selvaganesh et al. [157] found that the stability and catalytic activity of Pt also get improved by incorporation of TiO_2. TiO_2 incorporation, in fact, helps in mitigating the aggregation of Pt particles and protects the Nafion memebrane against peroxide radicals formed during the cathodic reduction of oxygen. The performance of $Pt\text{-}TiO_2/C$ degrades 10% after 5000 test cycles than 28% of Pt/C [158]. Huang et al [159] reported an enhanced ORR activity and durability with a Pt electrocatalyst supported

on a carbon-doped TiO_2 support (Pt/c-TiO_2/CNTs). It was claimed that under oxidizing conditions of 5000 potential cycles from 0.6- 1.0 V, Pt on c-TiO_2/CNTs suffered almost no loss in ORR activity while the commercial Pt/C catalyst undergoes more than 50% loss at 0.75 V. A similar electrocatalyst, $Pt/Nb_{0.06}Ti_{0.94}O_2$, was also examined [160] for its activity toward ORR. A monotonic increase in Pt ORR mass activity with increasing catalyst support's conductivity suggested that the support conductivity plays an important role in enhancing the catalyst mass activity.

Mono disperse dumbbell-like Pt-Fe_3O_4 NPs have been synthesized by epitaxial growth of Fe onto Pt NPs followed by Fe oxidation [161]. The NPs size in the structure is tunable from 2 to 8 nm for Pt and 6 to 20 nm for Fe_3O_4. Pt NPs in the Pt-Fe_3O_4 structure show a 20-fold increase in mass activity toward ORR compared with the single component Pt NPs and the commercial 3nm Pt particles.

Greeley et al [147] reported a new set of ORR electrocatalysts consisting of Pd or Pt alloyed with early transition metals such as Sc or Y. Their study showed that the activity of polycrystalline Pt_3Sc and Pt_3Y electrode is enhanced relative to pure Pt by a factor of 1.5-1.8 and 6-10, respectively, in the range of 0.9-0.87 V. These new electrodes were demonstrated by density functional theory calculations as being the most stable binary alloys with ORR activity likely to be better than Pt. Escudero-Escribano et al. [162] obtained a novel highly active and stable electrocatalysts, Pt_5Gd, for the ORR. The activity of this catalyst is found to be similar to that on previously reported Pt_3Y. The latter catalyst was claimed to be the most active Pt-based polycrystalline alloy for the ORR.

Kang and Morray [40] has recently described the low- temperature solution-phase synthesis of cubic Mn-Pt NCs (nanocrystals) and studied their ORR activities. To synthesize Mn-Pt NCs, $Pt(acac)_2$ was dissolved in benzyl ether or phenyl ether in presence of oleic acid and oleylamine and then injected a $Mn_2(CO)_{10}$ stock solution at 160 ºC followed by rapid heating of the solution to 200-205 ºC and kept the solution at this temperature for 30 min. The average edge length of as-synthesized Pt-Mn nanocubes was 7.7 nm. The combination of oleic acid and oleylamine was essential to obtain particles of uniform size and shape. The as-synthesized nanocubes were chemically disordered, with Mn and Pt in an fcc unit cell of the A1 phase. The nanocube structure was converted from the A1 phase to the ordered L12 phase ($AuCu_3$ structure) when annealed at 600 ºC for 30 min and were identified as $MnPt_3$ in consistent with the published result of Lee et al. [163]. Spherical Mn-Pt NCs, which are actually polyhedral enclosed by (100) and (111) facets, could also be synthesized by including $Mn_2(CO)_{10}$ as starting material instead of utilizing hot injection at 160 ºC. This synthesis of spherical Mn-Pt NCs synthesis is similar to those reported by Lee et al. [163] and Ono et al. [164]. The ORR study showed that the Mn-Pt nanocubes are more active than the commercial catalyst. Also, their catalytic properties are shape dependent.

With the aim to decrease the Pt loading and improve the ORR kinetics, Zhang et al. [66] developed a new class of the ORR catalysts with a high activity and very low metal content. They comprised of Pt monolayer deposited on the surface of carbon supported non-noble metal─noble metal core-shell NPs. The non-noble metal – noble metal core – shell NPs were synthesized as shown in figure 4. Pt monolayers were obtained on Au/Ni/C, Pd/Co/C, and Pt/Co/C substrates investigated for ORR activity using the RDE method. The mass activity of all the three Pt monolayer electrocatalysts was more than order of magnitude higher than that of a state-of-the art commercial Pt/C electrocatalyst. It is demonstrated that high-activity electrocatalysts can be devised that contain only a

fractional amount of Pt and very small amount of another noble metal. Guo et al. [165] designed Au/Pt hybrid electrocatalysts with sponge-like hollow structure (Figure 9).

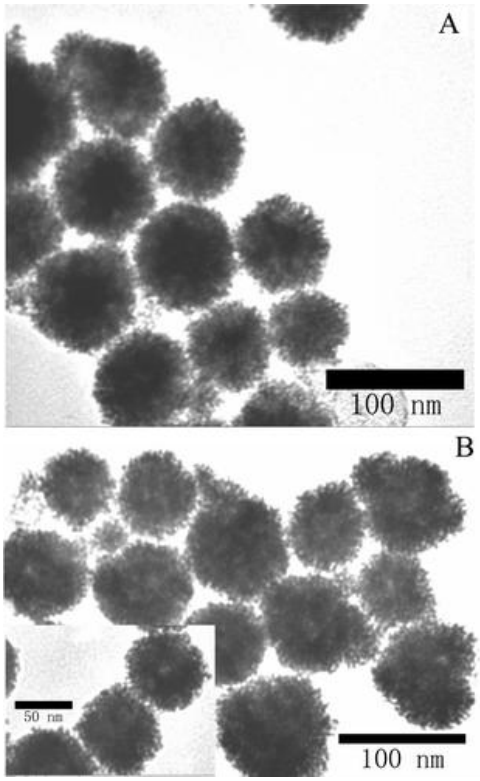

Figure 9. Typical TEM images of the as-prepared spongelike Au/Pt hybrid nanospheres at different magnifications. (Reprinted from ref. 165 by the permission from American Chemical Society).

This hybrid material is stated to be quite stable and low cost and exhibits higher catalytic activity for the ORR in O_2-saturated 0.5 M H_2SO_4. Similarly, carbon-supported Pt@Cu "core-shell" NPs synthesized by Sarkar and Manthiram [59] showed the ORR activity superior to commercial Pt catalyst, both per unit mass of Pt and per unit active surface area basis. Further, the surface area specific activities of novel electrodes increased linearly with increasing initial nominal Cu content. The increase in activity of ORR is ascribed to an electronic modification of the outer Pt shell by the Pt-Cu core. Also, a series of carbon-supported PdM@PdPt (M = Ni, Co, Fe, and Cr) NPs with similar particle sizes were prepared by an exchange reaction between PdM NPs and an aqueous solution of $PtCl_4^{2-}$ [166]. The activity of the ORR catalysts was evaluated in presence of 0.1 M methanol to test their selectivity for use in DMFCs. Results indicated that the commercial Pt/C catalysts lose 50% of their activity in the presence of 0.1 M methanol at 0.9 V while the PdM@PdPt/C catalysts retain more than 75% of their activity. Choi et al. [167] reported a designed synthesis of well defined Pd@Pt core-shell NPs with a controlled Pt shell thickness of 0.4-1.2 nm by a facile wet chemical method and investigated their electrocatalytic performances for ORR as a function of shell thickness. The Pd@Pt NPs with 0.94 nm Pt shells exhibited enhanced specific activity and higher durability compared to other Pd@Pt NPs and commercial Pt/C catalysts.

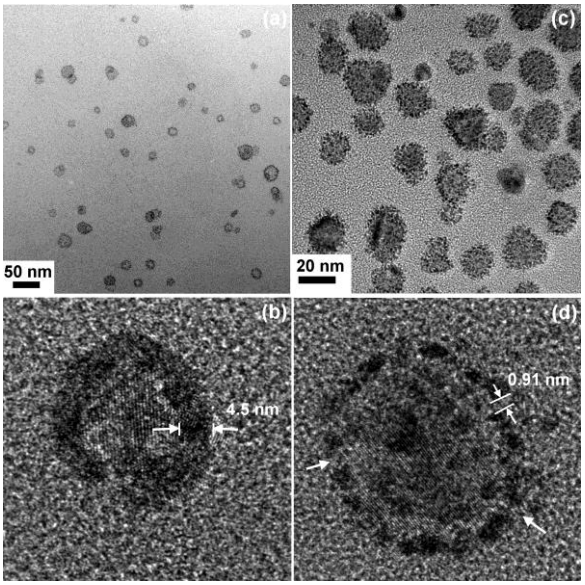

Figure 10. TEM micrographs of the hollow Ag−Pt nanoparticles (a,b) and hollow Pt shell with nanochannels (c,d). (Reprinted from ref. 23 by the permission from American Chemical Society).

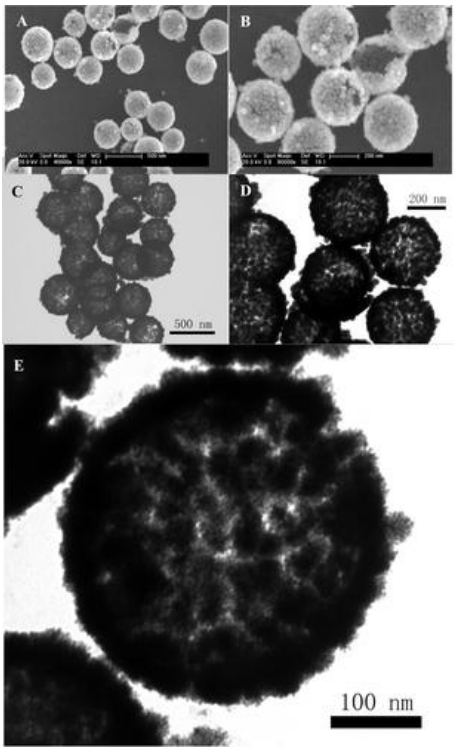

Figure 11. Typical SEM images (A, B) of RHAHS prepared at different magnifications (1% H_2PtCl_6: 1.5 mL); typical TEM images (C−E) of RHAHS prepared at different magnifications (1% H_2PtCl_6: 1.5 mL). (Reprinted from ref. 169 by the permission from American Chemical Society).

To produce Pt catalysts with a high surface area and high utilization efficiency, Chen et al. [23] developed a facile procedure for obtaining the hollow Pt nanosphere catalysts with nanochannels

(Figure 10). The latter catalysts, thus designed, provide the interior surface also for the catalytic reaction which leads to a higher surface area and hence the catalytic activity. On the other hand, Wen et al. [168] developed a facile template route of obtaining highly distributed core/shell Pt/C NPs into the nanochannels of MC (Pt@C/MC). Because of the combination of unique porous structure, high surface area, and uniformly dispersed Pt NPs, the as-synthesized Pt@C/MC not only show high activity and considerable stability for ORR but also present methanol-tolerant behaviour, which might be of great technological significance for developing methanol-tolerant cathodes in DMFCs. Guo et al [169] reported the synthesis of raspberry-like hierarchical Au/Pt NP assembling hollow spheres (RHAHS) with pore structure and complex morphology (Figure 11). This method is considered to be advantageous because of its simplicity, quickness, and good reproducibility. The as-prepared RHAHS exhibited ORR activity greater than that of commercial platinum black (CPB). The ORR follows a four-electron reduction of O_2 to H_2O in a 0.5 M air-saturated H_2SO_4 solution.

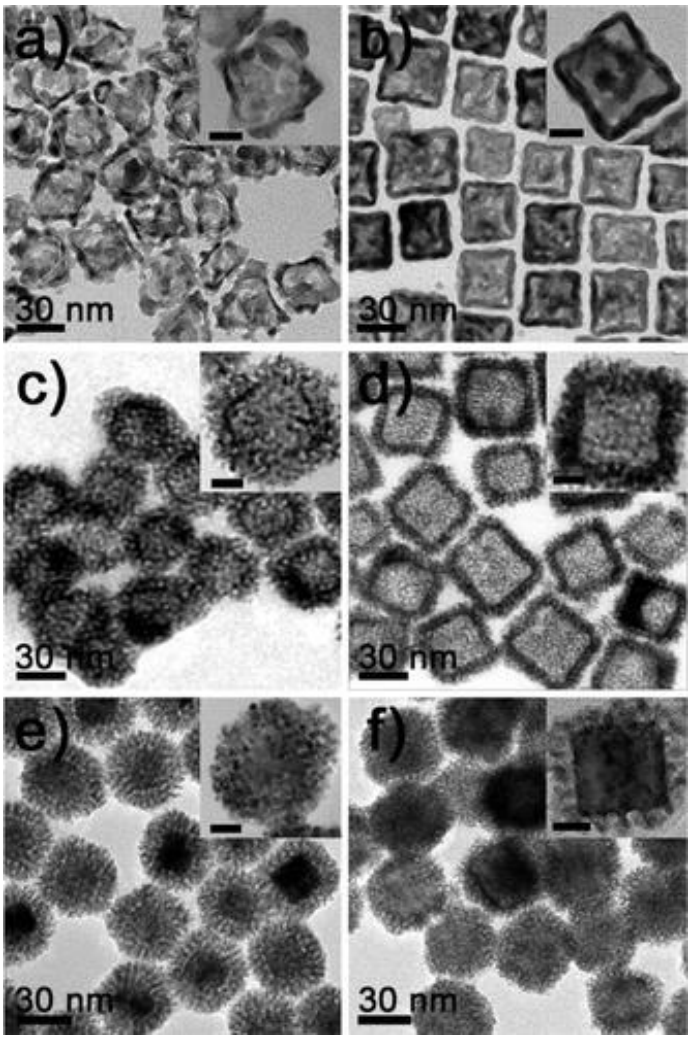

Figure 12 . TEM images of (a) octahedral nanocages, (b) cubic nanocages, (c) octahedral dendritic hollow nanocages, (d) cubic dendritic hollow nanocages, (e) octahedral dendritic nanocages, and (f) cubic dendritic nanocages. High-magnification TEM images are shown in each inset. Scale bars in the insets indicate 10 nm. (Reprinted from ref. 170 by the permission from American Chemical Society).

Godinez-Salomon et al. [53] studied the ORR on Ni@Pt core-shell nanocatalyst in acid media and observed that the Ni@Pt NPs, before and after thermal treatment, have more than twice enhanced catalytic activity than Pt NPS synthesized by the same way. Hong et al. [170] prepared the Pd-Pt bimetallic alloy NCs with hollow structures and dendritic Pd@Pt core-shell NCs could be selectively synthesized by a galvanic replacement method with Pd NCs with different morphologies as sacrificial templates (Figure 12). The hollow NCs exhibited considerably enhanced ORR activities compared to those of Pd@Pt core-shell NCs.

Kuttiyiel et al. [171] reported a new promising route to the development of novel core-shell catalysts with substantial reduction in Pt loading while retaining high ORR activity and stability. Electrochemistry and DFT methods revealed that the high ORR activity and durability of PtNiN catalyst is attributed to Ni nitride core, modifying the behavior of Pt shell by inducing both geometric and electronic effects. The PtNiN synthesis involves nitriding Ni NPs and simultaneously encapsulating it by 2-4 monolayer-thick Pt shell.

Peng et al. [24] prepared Pt-on-Ag bimetallic NPs based on a heterogeneous nucleation and growth method. Pt hollows can be produced from Pt-on-Ag NPs through the dissolution of Ag metal cores as shown in figure 2. The carbon-supported Pt hollow catalysts have much higher ORR activity than the Pt-on-Ag NPs or commercial Pt catalyst (E-tek, 20% Pt). Ma et al. [22] prepared ultra-low Pt catalysts with Pt_{shell} - Au_{core} nanostructure by seed mediate method. The Pt/Au/C (Pt : Au = 3:2, Pt + Au = 4wt%) catalyst exhibited attractive ORR activity in both electrochemical test and single cell test.

Qu et al. [172] designed a new particle-on-alloy nanostructured material, in which Pt particles are supported by an amorphous NiCo alloy. The Pt-on-NiCo nanostructures were synthesized through the artificial active template collodion membrane by one step method. The optimized Pt_{53}-on-NiCo nanostructures have improved both ORR activity and stability of electrocatalyst in 0.5 M H_2SO_4, relative to the commercial Pt stable with a loss of only ~ 8% initial EASA and a small degradation of 5 mV in the half-wave potential after 30,000-cycles test. However, the commercial Pt catalyst lost ~ 26% of the initial EASA and showed a large decrease of 28 mV in the half-wave potential after the same examination. It is considered that the low OH_{ads} coverage on the surface of Pt-on-NiCo nanostructures improves the kinetics of ORR, resulting in the higher activity toward ORR.

Very recently, Zhu et al. [173] synthesized a new class of 20 nm x 2 nm ternary alloy FePtM (M = Cu, Ni) nano rods (NRs) with controlled composition. When these alloys (supported on carbon) treated with acetic acid (AA) and then electrochemical etching in 0.1 M $HClO_4$, were transformed into core/ shell FePtM/Pt NRs (Figure 13). These core/shell NRs, especially FePtCu/Pt NRs, exhibited much improved ORR activity and durability.

Guo et al. [174] reported a new seed-mediated synthesiss of core/shell FePtM/FePt (M = Pd, Au) nanowires (NWs) and their electrocatalysis for ORR in 0.1 M $HClO_4$. These FePtM/FePt NWs show shell thickness and core composition-dependent electrocatalytic activity for ORR. They are generally more active and durable than the corresponding alloy NW. The FePtM/FePt (0.8 nm shell) NWs are also stable in the ORR condition and show no activity decrease after 50000 potential sweeps between 0.4 and 0.8 V (vs. Ag/AgCl). Authors have claimed that these are the most efficient catalysts ever reported for ORR.

Ge et al. [175] fabricated a novel nanoporous Pt-Cu bimetallic catalyst with a Pt skin and Pt-Cu core by electrochemically dealloying a bulk Pt-Cu binary alloy using a potential controlled approach. The Pt/Cu ratio of the dealloyed nanoporous catalyst can be readily adjusted in a wide composition range by only controlling dealloying potential. With optimal composition, the dealloyed nanoporous Pt-Cu catalyst possesses enhanced catalytic activity towards ORR in comparison with the commercial Pt/C catalyst.

Gumeci et al. [176] reported the synthesis of $PtCu_3$ bimetallic NPs via a sonochemical method. The catalysts so obtained were activated using an electrochemical dealloying procedure to prepare an ORR electrocatalysts. The dealloyed catalyst consisted of a Pt-rich surface layer, over a core of a Pt_3Cu composition. The dealloyed sample exhibited ~3 to 6 fold enhancement in ORR activity when compared to commercial Pt catalysts.

It is known that the particle size increases with increasing metal loading on the carbon support. Commercial amorphous carbon has low surface area of less than $300m^2g^{-1}$ and so, high metal dispersion, particularly at high metal loadings such as 50% or so is difficult to obtain. However, the GNS (graphene nano-sheet) support (specific surface area ca. $2630m^2g^{-1}$) can accommodate Pt loadings of 50wt% [9] and can be used as an excellent support to synthesize small and uniformly dispersed Pt or Pd NPs. A graphene sheet, a two dimensional carbon material with single (or a few) atomic layer, has attracted great attention for both fundamental science and applied research. Seo et al. [177] obtained GNS-supported Pt (Pt/GNS) and Pd (Pd/GNS) NPs and observed superior ORR activity of Pd/GNS compared to Pt/GNS in alkaline media. Kou et al. [41] studied the ORR on Pt NPs supported on functionalized graphene sheets (f-GNS) in 0.5 M H_2SO_4. This electrode showed a higher electrochemical surface area and oxygen reduction activity with improved stability as compared with the commercial catalyst. The improved performance can be attributed to smaller particle size (~2 nm) and less aggregation of Pt NPs on the functionalized graphene sheets.

Xin et al. [178] deposited the Pt NPs onto graphene sheets via synchronous reduction of H_2PtCl_6 and graphene oxide (GO) suspension using $NaBH_4$. Lyophilization is introduced to avoid irreversible aggregation of GNS, which happens during conventional drying process. Pt/GNS catalysts reveal a high catalytic activity for both methanol oxidation and oxygen reduction reaction compared to Pt supported on carbon black (Pt/C). The performance of the catalytic film is further improved after heat treatment in N_2 atmosphere at 300 ºC for 2h. In fact, the interaction between GNS and Pt NPs is enhanced during annealing. Rao et al. [179] prepared graphene-supported Pt and Pt_3M (M = Co and Cr) alloy NPs by ethylene glycol reduction method. The ORR activity of Pt_3M/GNS electrode is found to be 3-4 times higher than that of Pt/GNS. In addition, Pt_3M/GNS electrodes exhibited overpotential 45-70 mV lower than that of Pt/GNS. The high catalytic performance of Pt_3M alloys is ascribed to the inhibition of formation of (hydr)oxy species on Pt surface by the alloying elements.

The ORR at acid treated graphene supported Pt-Ni alloy NPs was studied, and the alloy catalyst had higher ORR activity than that at pure Pt catalysts in both acidic and alkaline solutions. The Pt-Ni alloy NPs were spherical and the size decreased slightly after acid treatment because of the dissolution of Ni atom. The binding energy of Pt upshifted after alloying and upshifted more after acid treatment. These changes in geometric and electronic structure were beneficial for ORR. The ORR followed the order: acid-treated Pt-Ni alloy > Pt-Ni alloy > Pt for both in acidic and alkaline solutions [180].

Recently, it is reported [181] that seven-nanometer FePt NPs obtained on GNS by a solution-phase self-assembly method exhibited higher ORR activity and durability in 0.1 M $HClO_4$ than the same NPs or commercial Pt NPs deposited on conventional carbon support. The GNS/FePt NPs annealed at 100 ^{0}C for 1 h under Ar + 5% H_2 exhibited specific ORR activities of 1.6 mA cm^{-2} at 0.512 V and 0.616 mA cm^{-2} at 0.557 V (vs Ag/AgCl) while the commercial Pt NPs (2-3 nm) had specific activities of 0.271 and 0.07 mA cm^{-2} at the same potentials. The GNS/FePt electrode showed nearly no activity change after 10,000 potential sweeps. Thus, the results clearly demonstrate that GNS is indeed a promising support to improve NP activity and durability for practical catalytic applications.

Hung and coworkers [182] prepared sulfonated GNS-supported Pt (s-Pt/GNS) electrocatalyst via a simple thermal-treatment in the presence of concentrated sulfuric acid for ORR in alkaline fuel cell and found 193% increase in the current density as compared with the Pt/GNS catalyst. He et al. [183] synthesized graphene nano-sheets supporting Pt NPs using perfulorosulfonic acid (PFSA) as a functionalized anchoring agent. The prepared Pt NPs are uniformly deposited on GNS with a narrow particle size ranging from 1-4 nm in diameter. The novel catalyst exhibited a higher catalytic activity for ORR. The PFSA/functionalized Pt/GNS (PFSA-Pt/GNS) catalyst revealed a better CO-oxidation and lower loss rate of electrochemical area in comparison with that of the plain Pt/GNS and conventional Pt/C catalyst. The PtCo NP catalysts on hexadecyltrimethylammonium bromide (CTAB)-functionalized graphene support [184], Pt NPs-dispersed GNS-wrapped MWCNT composites [185], and Pt/GNS/CB composite structure [186], recently investigated have also shown considerably enhanced ORR activities, specific surface areas and long term durabilities compared to commercial catalysts.

Sebastian et al. [187] prepared Pt catalysts-supported on carbon nanofibers (CNFs) and observed an enhanced ORR activity and durability in 0.5 M H_2SO_4. The CNF synthesized at 650 ºC showed the better ORR performance than those synthesized at 550 and 700 ºC. Wu et al. [188] designed a novel electrode, Pt nano-dendrites anchored on bamboo-shaped carbon nanofiber arrays (CNFAs) (Pt NDs/CNFAs) and demonstrated as highly efficient ORR elecrocatalysts in O_2-saturated 0.1 M $HClO_4$. This novel electrode was designed by growing vertically CNFAs on carbon paper via plasma enhanced chemical vapour deposition, followed by the direct synthesis of Pt nanodendrites using a simple surfactant-free aqueous solution method. The ORR on Pt nanodendrites /CNFAs followed a 4 electron pathway.

Masuda et al. [189] prepared the Pt-CeO_x/C catalyst by a combined process of precipitation and co-impregnation methods and have clearly shown that the enhancement of ORR activity can be attributed to the inhibition of Pt oxide formation by the CeO_x layer, of which Ce^{3+} was oxidized to Ce^{4+} instead of Pt at Pt oxide formation potential. The Pt/Ir-IrO_2 electrocatalyst also showed much higher ORR activity than that of Pt/IrO_2 electrocatalyst in 0.5 M H_2SO_4. Life tests revealed that Pt/Ir-IrO_2 exhibits excellent stability [190]. The superior ORR activities were also reported for $Pt_{0.55}Pd_{0.45}$/ C-$Nb_{0.07}Ti_{0.93}O_2$ [191], $Co_6Mo_6C_2$/GCB (graphitized carbon black) [192], meso-structured Pt thin film on carbon [193] in acid solutions. Altamirano-GutierreZ et al. [194] investigated Pt-CeO (1:1) and Pt-Pd (1:1) as the cathodes for the alkaline direct fuel cells. In presence of methanol, the Pt-CeO_2 nanocatalyst demonstrated significantly higher selectivity and tolerance capability to the alcohol than Pt and Pt-Pd.

Very recently, Lee et al. [51] attempted to control and significantly improve ORR performance through a reversible surface segregation of Pt in Pt_3Au/C catalysts. The surface segregation and the reverse surface segregation of Pt were realized through heat treatments of Pt_3Au/C catalysts in CO and Ar atmospheres, respectively. All of the Pt_3Au/C catalysts exhibited improved ORR performance compared to that of Pt/C, and the CO treated Pt_3Au/C exhibited the best performance. The improved ORR performance of the Pt_3Au/C catalysts might be attributed to OH^- repulsive properties of the surfaces.

Fu et al. [195] reported one- pot water-based synthesis of Pt-Pd alloy (A) nanoflowers (NFs) and their superior ORR activity and remarkable methanol tolerant ability in acid media. The electrocatalytic activity and stability of the Pt-Pd ANFs for the ORR were superior in 0.1 M $HClO_4$ solution. On the other hand, Alia et al. [196] prepared Pt coated Cu NWs (Pt/CuNWs) and Pt nanotubes as ORR electrocatalysts and examined them in 0.1M $HClO_4$. Pt/CuNW catalysts showed ORR activities of 1.5 mA cm^{-2}, significantly greater than Pt/C or silver templated PtNTs (Ag). Durability tests indicated improved retention of EASA and ORR activity in comparison to Pt/C.

Alia et al. [197] synthesized Pt-coated palladium nanotubes (Pt/Pd NTs) via the partial galvanic displacement of Pd nanotubes. Pt coatings were controlled to a loading of 9 (PtPd 9), 14(PtPd 14), and 18 (PtPd 18) wt%, respectively. The ORR experiments have been used to evaluate the activities of Pt/PdNTs, Pt nanotubes, Pd nanotubes, and supported Pt NPs for PEMFC cathodes. The dollar (10.4 $A\$^{-1}$) and area (specific surface area) normalized ORR activities of Pt/ PdNTs exceeds the United States Department of Energy (DOE) targets. PtPd9 exceeds the DOE dollar activity target (9.7 $A\$^{-1}$) by 7% and it exceeds the specific area activity target by 40-43%. Du et al. [49] reported a simple one-pot synthesis of PtNi-MWCNT hybrid nanostructures. The catalysts, so obtained, have significantly higher activities towards ORR than the state-of-the-art TKK Pt/C. The specific and mass activities are 1.065 mA cm^{-2} and 0.51A mg_{Pt}^{-1}, respectively. Thus, the mass activity of PtNi-MWCNT surpasses the DOE mass activity target of 0.44 A mg_{Pt}^{-1}. This catalyst retained a greater proportion of EASA and ORR activity than Pt/C after durability test.

2. CONCLUSIONS

The research work carried out during recent years with aimed at to decrease the mass and increase the percentage utilization efficiency and hence the activity of platinum toward the ORR has been comprehensively reviewed in the present article. Platinum has been alloyed with a number of transition metals such as Sc, Y, Cr, Mn, Fe, Co, Ni, Cu, Ir, Ru, Rh, Pd, Au, etc. and produced in highly dispersed forms on high surface area carbon supports. Varied carbon support materials namely activated carbon, carbon black, graphitized carbon black, carbon nanofibers, bamboo-shaped carbon nanofiber arrays (CNFAs), carbon nanotubes, graphene, functionalized graphene, GNS-wrapped MWCN, etc have been used. Also, Pt cathode materials have been designed as core-shells, hollow nanospheres with nanochannels, raspberry-like hierarchical Au/Pt NP assembling hollow spheres (RHAHS)**,** etc., requiring sufficiently reduced mass and enhanced percentage utilization efficiency. The Ru@Pt core-shell catalyst did not indicate any degradation after 1000 cycles in 0.1 M $HClO_4$. The

RHAHS-modified electrode displayed ~ 8 times higher ORR activity compared to commercial platinum black (CPB) in 0.5 M H_2SO_4. The specific surface area and specific activity of Pt-coated palladium nanotubes designed recently are reported to exceed the United States Department of Energy (DOE) targets of 7% and 9.7 A $\$^{-1}$, respectively. Further, the crystallite size of Pt has been reduced to 1-5 nm through suitable design of the catalysts. Studies presented in this report show that the electrocatalytic properties of the nanostructured Pt alloy catalysts depend upon a number of preparation variables such as electrode design, preparation method, experimental condition (temperature, pH, etc), alloy composition, nature of precursor, and thermal treatment. It seems, therefore, possible to develop cost-effective catalyst to meet the requirements for fuel cell commercialization through a proper control of these catalyst preparation variables. To achieve the objective, the future work is desired to focus mainly on: (i) optimization of the geometry, composition and structure of already discovered active Pt alloys to improve further their catalytic activity and stability, (ii) application of graphene, functionalized graphene, and graphene-CNTs composites as support materials and (iii) development and optimization of new cost-effective catalyst designs and their synthetic procedures for fuel cell application.

ACKNOWLEDGEMENT
Authors thank the Council of Scientific and Industrial Research (CSIR), New Delhi for the award of the financial support (Ref. No. 01/2747/13/EMR-II).

References

1. K. Scott and A. K. Shukla, *Modern Aspects of Electrochem.*, 40 (2007) 127.
2. E. Antolini and E. R. Gonzalez, *J. Power Sources*, 195 (2010) 3431.
3. R.N. Singh, Madhu and R. Awasthi. *Alcohol Fuel Cells* (Chapter 16) in (Edited by Prof. S.L. Suib), Elsevier, July' 2013, p. 453-478 (ISBN: 978-0-444-53880-2).
4. E. H. Yu, U. Krewer and K. Scott, *Energies*, 3 (2010)1499.
5. C. Lamy, A. Lima, V. LeRhun, F. Delime, C. Coutanceau and J. Léger, *J. Power Sources*, 105 (2002) 283.
6. C. Bianchini and P. K. Shen, *Chem. Rev.*, 109 (2009) 4183.
7. R. Awasthi and R. N. Singh, *Int. J. Hydrogen Energy*, 37 (2012) 2103.
8. R. Awasthi and R. N.Singh, *Int. J. Electrochem. Sci.*, 6 (2011) 4775.
9. R.N.Singh and R. Awasthi, *Catal. Sci. Tech.*, 1 (2011) 778.
10. Y. Z. Su, M.-Z. Zhang, X. B. Liu, Z. Y. Li, X. C. Zhu, C. W. Xu and S. P. Jiang, *Int. J. Electrochem. Sci.*, 7 (2012) 4158.
11. C. Jin, Y. Song and Z. Chen, *Electrochim. Acta*, 54 (2009) 4136.
12. Y. Zhu, S. Y. Ha and R. I. Masel, *J. Power Sources*, 130 (2004) 8.
13. J. Yeom, R. S. Jayashree, C, Rastogi, M. A. Shannon, P. J. A. Kanis, *J. Power Sources*, 160 (2006) 1058.
14. R. N. Singh, A. Singh and Anindita, *Carbon*, 34 (2009) 2052.
15. Madhu, C. S. Sharma and R. N. Singh, *Electrocatal.*, DOI: 10.1007/s12678-013-0141-6.
16. Y. Su, C. Xu, J. Liu and Z. Liu, *J. Power Sources*, 152 (2005) 1.
17. T. Lopes, E. Antolini and E. R. Gonzalez, *Int. J. Hydrogen Energy*, 33 (2008) 5563.
18. D. Morales-Acosta, L. G. Arriaga, L. Alvarez-Contreras, S. Fraire Luna and F. J. Rodríguez Varela, *Electrochem. Commun.*, 11 (2009) 1414.

19. T. T. Cheng and E. L. Gyenge, *J. Appl. Electrochem.*, 39 (2009) 1925.
20. E. Antolini, T. Lopes and E. R. Gonzalez, *J. Alloys Compd.*, 461 (2008) 253.
21. N. M. Markovic, T. J. Schmidt, V. Stamenkovic and P. N. Ross, *Fuel cell*, 1 (2001) 105.
22. Y. Ma, H. Zhang, H. Zhong, T. Xu, H. Jin and X. Geng, *Catal. Commun.*, 11 (2010) 434.
23. H. M. Chen, R. S. Liu, M. Y. Lo, S. C. Chang, L. D. Tsai, Y. M. Peng and J. F. Lee, *Phys. Chem. C Lett.*, 112 (2008) 7522.
24. Z. Peng, J. Wu and H. Yang, *Chem. Mater.*, 22 (2010) 1098.
25. R. Othman, A. L. Dicks and Z. Zhu, *Int. J. Hydrogen Energy*, 37 (2012) 357.
26. F. Cheng, Y. Su, J. Liang, Z. Tao and J. Chen, *Chem. Mater.*, 22 (2010) 898.
27. Q. Liu, J. Jin and J. Zhang, *Appl. Mater. Interfaces*, 12 (2013) 5002.
28. S. Pylypenko, S. Mukherjee, T. S. Olson and P. Atanassov, *Electrochim. Acta*, 53 (2008) 7875.
29. Y. Liang, Y. Li, H. Wang, J. Zhou, J. Wang, T. Regier and H. Dai, *J. Am. Chem. Soc.*, 134 (2012) 3517.
30. Y. Liang, Y. Li, H. Wang, J. Zhou, J. Wang, T. Regier and H. Dai, *Nat. Mater.*, 10 (2011) 780.
31. Madhu and R. N. Singh, *Int. J. Hydrogen Energy*, 36 (2011) 10006.
32. R. N. Singh and C. S. Sharma, *Eng. Technol. Appl. Sci. Res.*, 2 (2012) 295.
33. C. S. Sharma, R. Awasthi, R. N. Singh and A. S. K. Sinha, *Phys. Chem. Chem. Phys.*, 15 (2013) 2033; *Electrochim. Acta, (2014), http://dx.doi.org/10.1016/j.electacta.2014.05.084*.
34. Madhu, C. S. Sharma and R. N. Singh, *Indian J. Chem.*, 52A (2013) 1383.
35. A. K. Shukla and R. K. Raman, *Annu. Rev. Mater. Res.*, 33 (2003) 155.
36. H. S. Wroblowa, Y. C. Pan and G. Razumney, *J. Electroanal. Chem.*, 69 (1976) 195.
37. H. A. Gasteiger, S. S. Kocha, B. Sompalli and F. T. Wagner, *Appl. Catal. B: Environ.*, 56 (2005) 9.
38. B. Viswanathan, C. V. Rao and U.V. Varadaraju, *Photo/Electrochem. Photobiol. Environm., Energy and Fuel*, 43-101, (2006).
39. J. W. Lee and B. N. Popov, *J. solid State Electrochem.*, 11 (2007) 355.
40. Y. Kang and C. B. Murray, *J. Am. Chem. Soc.*, 132 (2010) 7568.
41. R. Kou, Y. Shao, D. Wang, M. H. Engelhard, J. H. Kwak, J. Wang,V. V. Viswanathan, C. Wang, Y. Lin, Y. Wang, I. A. Aksay and Jun Liu, *Electrochem. Commn.*, 11 (2009) 954.
42. J. Zhao and A. Manthiram, *Appl. Catal. B: Environ.*, 101 (2011) 660.
43. D. Banham, F. Feng, T. Fürstenhaupt, K. Pei, S. Ye and V. Birss, *J. Power Sources*, 196 (2011) 5438.
44. Z. Xu, H. Zhang, S. Liu, B. Zhang, H. Zhong and D. S. Su, *Int. J. Hydrogen Energy*. 37 (2012) 17978.
45. D. Banham, F. Feng, K. Pei, S. Ye and V. Birss, *J. Mater. Chem. A*, 1 (2013) 2812.
46. C. Alegre, M. E. Gálvez, R. Moliner, V. Baglio, A. S. Aricò and M. J. Lázaro, *Appl. Catal. B: Environ.*, 147 (2014) 947.
47. Y. Tang, F. Gao, S. Yu, Z. Li and Y. Zhao, *J. Power Sources*, 239 (2013) 374.
48. A. C. Garcia and E. A. Ticianelli, *Electrochim. Acta*, 106 (2013) 453.
49. S. Du, Y. Lu, S. K. Malladi, Q. Xu and R. Steinberger-Wilckens, *J. Mater. Chem. A*, 2 (2014) 692.
50. M. Rahsepar, M. Pakshir and H. Kim, *Electrochimica. Acta*, 108 (2013) 769.
51. K. S. Lee, H. Y. Park, H. C. Ham, S. J. Yoo, H. J. Kim, E. Cho, A. Manthiram and J. H. Jang, *J. Phys. Chem. C*, 117 (2013) 9164.
52. R. Loukrakpam, J. Luo, T. He, Y. Chen, Z. Xu, P. N. Njoki, B. N. Wanjala, B. Fang, D. Mott, J. Yin, J. Klar, B. Powell and C. J. Zhong, *J. Phys. Chem. C*, 115 (2011) 1682.
53. F. G. Salomón, M. H. López and O. Feria, *Int. J. Hydrogen Energy*, 37 (2012) 14902.
54. A. P. Oleg, *J. Solid State Electrochem.*, 12 (2008) 609.
55. H. Liu, C. Song, L. Zhang, J. Zhang, H. Wang and D. P. Wilkinson, *J. Power Sources*, 155 (2006) 95.

56. C. D. Stassi, V. Baglio, A. Di Blasi, V. Antonucci, A. S. Arico, A. M. Castro Luna, A. Bonsei and W. E. Triaca, *J. Appl. Electrochem.*, 36 (2006) 1143.
57. Q. He and S. Mukerjee, *Electrochem. Acta*, 55 (2010) 1709.
58. Y. Qian, W. Wen, P. A. Adcock, Z. Jiang, N. Hakim, M. S. Saha and Sanjeev Mukerjee, *J. Phys. Chem. C*, 112 (2008) 1146.
59. A. Sarakar and A. manthiram, *J. Phys. Chem. C*, 114 (2010) 4725.
60. Z. M. Peng, H. J. You and H. Yang, *Adv. Fun. Mater.*, 20 (2010) 3734.
61. R. Srivastava, P. Mani, N. Hahn and P. Strasser, *Angew. Chem., Int. Ed*, 46 (2007) 8988.
62. J. Zhang, Y. Mo, M. B. Vukmirovic, R. Klie, K. Sasaki, and R. R. Adzic, *J Phys. Chem. B.*, 108 (2004) 10955.
63. X. Cui, S.Wu, S. Jungwirth, Z. Chen, Z. Wang, L. Wang and Y. Li, *Nanotechn.*,24 (2013) 295402
64. D. F. Yancey, E. V. Carino, and R. M. Crooks, *J. Am. Chem. Soc.*,132 (2010) 10988.
65. S. R. Brankovic, J. X. Wang and R. R. Adzic, Surf. Sci., 477 (2001) L173.
66. J. Zhang , F. H. B. Lima , M. H. Shao , K. Sasaki ,J. X. Wang ,J. Hanson and R. R. Adzic, *J Phys. Chem. B.*, 109 (2005) 22701.
67. M. Shao, K. Sasaki, N. S. Marinkovic, L. Zhang and R. R. Adzic, *Electrochem. Commun.* 9 (2007) 2848.
68. K. Sasaki, H. Naohara, Y. Cai, Y. M. Choi, P. Liu, M. B. Vukmirovic, J. X. Wang and R. R. Adzic, *Angew. Chem. Int. Ed.*, 49 (2010) 8602 .
69. J. Qu, H. Liu, F. Ye, W. Hu and J. Yang, *Int. J. Hydrogen Energy*, 37 (2012) 13191.
70. C. Wang, D. Vliet, K. C. Chang, H. You, D. Strmcnik, J. A. Schlueter, N. M. Markovic and V. R. Stamenkovic, *J. Phys. Chem. C*,113 (2009) 19365.
71. M. K. Carpenter, T. E. Moylan, R. S. Kukreja, M. H. Atwan and M. M. Tessema, *J. Am. Chem. Soc.*, 134 (2012) 8535.
72. A. Jackson, V. Viswanathan, A. J. Forman, A. H. Larsen, J. K. Nørskov and T. F. Jaramillo, *Chem. ElectroChem.*, 1 (2014) 67.
73. L. Gan, M. Heggen, S. Rudi and P. Strasser, *Nano Lett.*, 12 (10) (2012) 5423.
74. C. W. B. Bezerra, L. Zhang, H. Liu, K. Lee, A. L. B. Marques, E. P. Marques, H. Wang and J. Zhang, *J. Power Sources*, 173 (2007) 891.
75. S. V. Selvaganesh, G. Selvarani, P. Sridhar, S. Pitchumani and A. K. Shukla, *Fuel Cell*, 11 (2011) 372.
76. D. S. Cameron, S. J. Cooper, I. L. Dodgson, B. Harrison and J. W. Jenkins, *Catal. Today*, 7 (1990) 113.
77. E. Antolini, *Appl. Catal. B: Environm.*, 88 (2009) 1.
78. A. Guha, W. Lu, T. A. Zawodzinski Jr. and D. A. Schiraldi, *Carbon*, 45 (2007) 1506.
79. E. Auer, A. Freund, J. Pietsch and T. Tacke, *Appl. Catal. A: Gen.*, 173 (1998) 259.
80. J. G. Oh, H. S. Oh, W. H. Lee and H. Kim, *J. Mater. Chem.*, 22 (2012) 15215.
81. E. Antolini, J. R. C. Salgado, L. G. R. A. Santos, G. Garcia, E. Pastor, E. A. Ticianelli and E. R. Gonzalez, *J. Appl. Electrochem.*, 36 (2006) 355.
82. N. M. Markovic and P. N. Ross, *Surf. Sci. Rep.*, 45 (2002) 117.
83. H. A. Gasteiger, N. Marković, P. N. Ross and E. J. Cairns, *Electrochim. Acta*, 39 (1994) 1825.
84. E. Antolini, *Mater. Chem. Phys.*, 78 (2003) 563.
85. H. Yang, N. Alonso Vante, C. Lamy and D. L. Akins, *J. Electrochem. Soc.*, 152 (2005) A704.
86. H. Yang, N. Alonso-Vante, J.-M. Léger and C. Lamy, *J. Phys. Chem. B*, 108 (2004) 1938.
87. R. C. Koffi, C. Coutanceau, E. Garnier, J.-M. Léger and C. Lamy, *Electrochim. Acta*, 50 (2005) 4117.
88. A. K. Shukla, R. K. Raman, N. A. Choudhury, K. R. Priolkar, P. R. Sarode, S. Emura and R. Kumashiro, *J. Electroanal. Chem.*, 563 (2004) 181.
89. R. K. Raman, G. Murgia and A. K. Shukla, *J. Appl. Electrochem.*, 34 (2004)1029.
90. W. Yuan, K. Scott and H. Cheng, *J. Power Sources*, 163 (2006) 323.

91. K. Scott, W. Yuan and H. Cheng, *J. Appl. Electrochem.,* 37 (2007) 21.
92. A. Fortunelli and A. M. Velasco, *J. Mol. Struct. Theochem.,* 586 (2002) 17.
93. W. Chen, J. Kim, S. Sun, and S. Chen, *J. Phys. Chem. C*, 112 (2008) 3891.
94. L. Xiong and A. Manthiram. *Electrochim. Acta,* 50 (2005) 2323.
95. F. H. B. Lima, M. J. Giz and E. A. Ticianelli, *J. Braz. Chem. Soc.,* 16 (2005) 328.
96. J. R. C. Salgado, E. Antolini, and E. R. Gonzalez, *Appl. Catal. B: Environm.,* 57 (2005) 283.
97. S. Siracusano, A. Stassi, V. Baglio, A. S. Aricò, F. Capitanio and A. C. Tavares, *Electrochim. Acta,* 54 (2009) 4844.
98. C. Wang, G. Wang, D. Vliet, K. C. Chang, N. M. Markovic and V. R. Stamenkovic, *Phys. Chem. Chem. Phys.*, 12 (2010) 6933.
99. X. Wang , F. Yuan, P. Hu , L. Yu and L. Bai. *J. Phys. Chem. C*, 113 (2009) 13456.
100. B. J. Hwang, S. M. S. Kumar, C. H. Chen, Monalisa, M. Y. Cheng, D. G. Liu and J. F. Lee, *J. Phys. Chem. C*, 111 (2007) 15267.
101. S. Dsoke, A. Moretti, G. Giuli and R. Marassi, *Int. J. Hydogen Energy*, 36 (2011) 8098.
102. K. Okaya, H. Yano, K. Kakinuma, M. Watanabe and H. Uchida, *ACS Appl. Mater. Inerfaces*, 4 (2012) 6982.
103. L. Yang, M. B. Vukmirovic, D. Su, K. Sasaki, J. A. Herron, M. Mavrikakis, S. Liao and R. R. Adzic, *J. Phys. Chem. C*, 117 (2013) 1748.
104. H. Yang, C. Coutanceau, J. M. Léger, N. Alonso-Vante and C. Lamy, *J. Electroanal. Chem.*, 576 (2005) 305.
105. J. F. Drillet, A. Ee, J. Friedemann, R. Kötz, B. Schnyder and V. M. Schmidt. *Electrochim. Acta*, 47 (2002) 1983.
106. E. Antolini, J. R. C. Salgado, A. M. dos Santos and E. R. Gonzalez, *Electrochem. Solid State Lett.,* 8 (2005) A226.
107. E. Antolini, J. R. C. Salgado and E. R. Gonzalez, *J. Power Sources,* 155 (2006) 161.
108. T. Y. Jeon, S. J. Yoo, Y. H. Cho, K. S. Lee, S. H. Kang and Y. E. Sung, *J. Phys. Chem. C*, 113 (2009) 19732.
109. A. Seo, J. Lee, K. Han and H. Kim, *Electrochim. Acta*, 52 (2006) 1603.
110. J. G. Oh, C. H. Lee and H. Kim, *Electrochem. Commun.,* 9 (2007) 2629.
111. J. Luo, N. Kariuki, L. Han, L. Wang, C. J. Zhong and T. He, *Electrochim. Acta*, 51 (2006) 4821.
112. A. Bonakdarpour, K. Stevens, G. D. Vernstrom, R. Atanasoski, A. K. Schmoeckel, M. K. Debe and J. R. Dahn, *Electrochim. Acta,* 53 (2007) 688.
113. F. Maillard, M. Martin, F. Gloaguen and J. M. Léger, *Electrochim. Acta,* 47 (2002) 3431.
114. V. Baglio, A. Stassi, A. Di Blasi, C. D'Urso, V. Antonucci and A. S. Aricò, *Electrochim. Acta,* 53 (2007)1360.
115. T. Toda, H. Igarashi, H. Uchida and M. Watanabe, *J. Electrochem. Soc.,* 146 (1999) 3750.
116. W. Li, W. Zhou, H. Li, Z. Zhou, B. Zhou, G. Sun and Q. Xin, *Electrochim. Acta,* 49 (2004) 1045.
117. M. Nesselberger, S. Ashton, J. C. Meier, I. Katsounaros, K. J. J. Mayrhofer and M. Arenz, *J. Am. Chem. Soc.*, 133 (2011) 17428.
118. M. Shao, A. Peles and K. Shoemaker, *Nano Lett.*, 11 (2011) 3714.
119. J. Zhang, H. Yang, J. Fang and S. Zou, Nano Lett., 10 (2010) 638.
120. J. Wu and H. Yang, *Nano Res.*, 4 (2011) 72.
121. S. W. Chou, J. J. Shyue, C. H. Chien, C. C. Chen, Y. Y. Chen and P. T. Chou, *Chem. Mater.*, 24 (2012) 2527.
122. H. Meng and P. K. Shen, *Chem. Comm.*, (2005) 4408.
123. H. Meng and P. K. Shen, *J. Phys. Chem. B*, 109 (2005) 22705.
124. N. Travitskya, T. Ripenbeina, D. Golodnitskya, Y. Rosenbergb, L. Burshteinb and E. Peleda, *J. Power Sources*, 161 (2006) 782.

125.N. R. Elezović, B. M. Babić, L. Gajić-Krstajić, P. Ercius, V. R. Radmilović, N. V. Krstajić and L. M. Vračar, *Electrochem. Acta*, 69 (2012) 239.
126.N. R. Elezovic, B. M. Babic, P. Ercius, V. R. Radmilovic, L. M. Vracar and N.V. Krstajic, *Appl. Catal. B*,125 (2012) 390.
127.C. K. Poh, S. H. Lim, Z. Tian, L. Lai, Y. P. Feng, Z. Shen and Ji. Lin, *Nano energy*, 2 (2013) 28.
128.J. Xu, G. Fu, Y. Tang, Y. Zhou, Y. Chen and T. Lu, *J. Mater. Chem.*, 22 (2012) 13585.
129.H. Yano, M. Kataoka, H. Yamashita, H. Uchida and M. Watanabe, *Langmuir*, 23 (2007) 6438.
130.G. Gupta, D. A. Slanac, P. Kumar, J. D. Wiggins-Camacho, X. Wang, S. Swinnea, K. L. More, S. Dai, K. J. Stevenson and K. P. Johnston, *Chem. Mater.*, 21 (2009) 4515.
131.C. V. Rao and B. Viswanathan, *J. Phys. Chem.*, 113 (2009) 18907.
132.A. Tegou, S. Papadimitrou, S. Armyyanov, E. Valova, G. Kokkinidis and S. Sotritopoulos, *J. Electroanal. Chem., 623* (2008) 187.
133.J. Zhang, K. Sasaki, E. Sutter and R. R. Adzic, *Science*, 315 (2007) 220.
134.J. Zhang , M. B. Vukmirovic , K. Sasaki , A. U. Nilekar , M. Mavrikakis and R. R. Adzic. *J. Am. Chem. Soc.*, 127 (2005) 12480.
135.M. B. Vukmirovic, J. Zhang, K. Sasaki, A. U. Nilekar, F. Uribe, M. Mavrikakis and R. R. Adzic. *Electrochim. Acta*, 52 (6) (2007) 2257.
136.A. U. Nilekar, Y. Xu, J. Zhang, M. B. Vukmirovic and K. Sasaki, *Top. Catal.*, 46 (2007) 276.
137.J. Wang, G. Yin, G. Wang, Z. Wang and Y. Gao, *Electrochem. Commun.*, 10 (2008) 831.
138.G. Selvarani, S. V. Selvaganesh, S. Krishnamurthy, G. V. M. Kiruthika, P. Sridhar, S. Pitchumani, and A. K. Shukla, *J. Phys. Chem. C*, 113 (2009) 7461.
139.C. Jeyabharathi, P. Venkateshkumar, J. Mathiyarasu and K. L. N. Phani, *Electrochim. Acta*, 54 (2008) 448.
140.W. Li, Q. Xin and Y. Yan, *Int. J. Hydrogen Energy*, 35 (2010) 2530.
141.M. Guerra-Balcázar, F. M. Cuevas-Muñiz, L. Álvarez-Contreras, L. G. Arriaga and J. Ledesma-García, *J. Power Sources*, 197 (2012) 121.
142.A. Sarkar, A. Vadivel Murugan and A. Manthiram, *Fuel Cells*, 10 (2010) 375.
143.H. Wang, J. Liang, L. Zhu, F. Peng, H. Yu and J. Yang, *Fuel cells*, 10 (2010) 99.
144.S. Ghosh, R. K. Sahu and C. R. Raj, *Nanotechn.*, 23 (2012) 385602.
145.Y. Wang, L. Zhang, F. Li and B. Gu, *Electrochim. Acta*, 102 (2013) 1.
146.K. Jukk, J. Kozlova, P. Ritslaid, V. Sammelselg, N. Alexeyeva and K. Tammeveski, *J. Electoranal. Chem.* 708 (2013) 31.
147.J. Greeley, I. E. L. Stephens, A. S. Bondarenko, T. P. Johansson, H. A. Hansen, T. F. Jaramillo, J. Rossmeisl, I. Chorkendorff and J. K. Nørskov, *Nat. Chem.*, 1 (2009) 552.
148.V. R. Stamenkovic, B. Fowler, B. S. Mun, G. Wang, P. N. Ross, C. A. Lucas and N. M. Marković, *Science*, 315 (2007) 493.
149.J. Kim, Y. Lee and S. Sun, *J. Am. Chem. Soc.*, 132 (2010) 4996.
150.S. Sun, C. B. Murray, D. Weller, L. Folks and A. Moser, *Science*, 287 (2000) 1989.
151.M. Chen , J. P. Liu and S. Sun, *J. Am. Chem. Soc.*, 126 (2004) 8394.
152.J. G. Oh and H. Kim, *J. Power Sources*, 181 (2008) 74.
153.S. Gao, H. Fan, X. Wei, L. Li, Y. Bando and D. Golberg, *Part. Part. Syst. Charact.* 30 (2013) 864.
154.M. N. Banis, S. Sun, X. Meng, Y. Zhang, Z. Wang, R. Li, M. Cai, T. K. Sham and X. Sun, *J. Phys. Chem. C*, 117 (2013) 15457.
155.J. Yin, L. Wang, C. Tian, T. Tan, G. Mu, L. Zhao and H. Fu, *Chem. Eur. J.* 19 (2013) 13979.
156.H. Inoue, K. Hosoya, N. Kannari and J. Ozaki, *J. Power Sources*, 220 (2012) 173.
157.S. V. Selvaganesh, G. Selvarani, P. Sridhar, S. Pitchumani and A. K. Shukla, *J. Electrochem. Soc.*, 159 (2012) B463.
158.S. V. Selvaganesh, G. Selvarani, P. Sridhar, S. Pitchumani and A. K. Shukla, *J. Electrochem. Soc.*, 157 (2010) B1000.
159.K. Huang, K. Sasaki, R. R. Adzic and Y. Xing, *J. Mater. Chem.*, 22 (2012) 16824.

160.Y.-J. Wang, D. P. Wilkinson and J. Zhang, *Dalton T.* 41 (2012) 1187.
161.C. Wang, H. Daimon and S. Sun, *Nano Lett.*, 9 (2009) 1493.
162.M. Escudero-Escribano, A. Verdaguer-Casadevall, P. Malacrida, U. Grønbjerg, B.P. Knudsen, A. K. Jepsen, J. Rossmeisl, I. E. Stephens and I. Chorkendorff, *J. Am. Chem. Soc.*, 134 (2012) 16476.
163.D. C. Lee , A. Ghezelbash , C. A. Stowell and B. A. Korgel , *J. Phys. Chem. B*, 110 (2006) 20906.
164.K. Ono, R. Okuda, Y. Ishii, S. Kamimura and M. Oshima, *J. Phys. Chem. B*, 107 (2003) 1941.
165.S. Guo, Y. Fang, S. Dong and E. Wang, *J. Phys. Chem. C*, 111 (2007) 17104.
166.Q. T. Trinh, J. Yang, J. Y. Lee and M. Saeys, *J. Catal.*, 291 (2012) 26.
167.R. Choi, S. Choi, C. H. Choi, K. M. Nam, S. Woo, J. T. Park and S. W. Han, *Chem. A Eur. J.*, 19 (2013) 8190.
168.Z. Wen, J. Liu and J. Li, *Adv. Mater.*, 20 (2008) 743.
169.S. Guo , S. Dong and E. Wang, *J. Phys. Chem. C*, 113 (2009) 5485.
170.J. W. Hong, S. W. Kang, B. S. Choi, D. Kim, S. B. Lee and S. W. Han, *ACS Nano*, 6 (2012) 2410.
171.K. A. Kuttiyiel, K. Sasaki, Y. M. Choi, D. Su, P. Liu, and R. R. Adzic, *Nano Lett.* 12 (2012) 6266.
172.Q. Qu, M. Wen, M. Cheng, A. Zhu, B. Kong and Y. Tian. *Int. J. Electrochem.*, 2012, doi:10.1155/2012/842048.
173.H. Zhu, S. Zhang, S. Guo, D. Su and S. Sun, *J. Am. Chem. Soc.* 135 (2013) 7130.
174.S. Guo,S. Zhang ,D. Su and S. Sun, *J. Am. Chem. Soc.* 135 (2013) 13879.
175.X. Ge, L. Chen, J. Kang, T. I. Fujita, A. Hirata, W. Zhang, J. Jiang and M. Chen, *Adv. Funct. Mater.* 23 (2013) 4156.
176.C. Gümeci, D. U. Cearnaigh, D. J. Casadonte and C. Korzeniewski, *J. Mater. Chem. A*, 1 (2013) 2322.
177.M. H. Seo, S. M. Choi, H. J. Kim and W. B. Kim, *Electrochem. Commun.*, 13 (2011) 182.
178.Y. Xin, J. Liua, Y. Zhoua, W. Liua, J. Gao, Y. Xie, Y. Yin and Z. Zoua, *J. Power Soureces*, 196 (2011) 1012.
179.C. V., Rao, A. L. M. Reddy, Y. Ishikawa and P. M. Ajayan, *Carbon*, 49 (2011) 931.
180.K. Zhang, Q. Yue, G. Chen, Y. Zhai, L. Wang, H. Wang, J. Zhao, J. Liu, J. Jia and H. Li, *J. Phys. Chem. C*, 115 (2011) 379.
181.S. Guo and S. Sun, *J. Am. Chem. Soc.*, 134 (2012) 2492.
182.T. F. Hung, B. Wang, C. W. Tsai, M. H. Tu, G. X. Wang, R. S. Liu, D. P. Tsai, M. Y. Lo, D. S. Shy and X. K. Xing, *Int. J. Hydrogen Energy*, 37 (2012) 14205.
183.D. He, K. Cheng, H. Li, T. Peng, F. Xu, S. Mu and Mu Pan, *Langmuir*, 28 (2012) 3979.
184.K.-W. Nam, J. Song, K. H. Oh, M.-J. Choo, H. Park, J.-K. Park and J. W. Choi, *Carbon*, 50 (2012) 3739.
185.S. S. J. Aravind and S. Ramaprabhu, *ACS Appl. Mater*. Interfaces 4 (2012) 3805.
186.Y. Li, Y. Li, E. Zhu, T. McLouth, C. Y. Chiu, X. Huang and Y. Huang, *J. Am. Chem. Soc.*, 134 (2012) 12326.
187.D. Sebastián, A. G. Ruíz, I. Suelves, R. Moliner, M. J. Lázaro, V. Baglio, A. Stassi and A. S. Aricò, *Appl. Catal. B*,115 (2012) 269.
188.R. Wu, Y. Xue, X. Qian, H. Liu, K. Zhou, S. H. Chan, J. N. Tey, J. Wei, B. Zhu and Y. Huang, *Int. J. Hydogen Energy*, 38 (2013) 16677.
189.T. Masuda, H. Fukumitsu, K. Fugane, H. Togasaki, D. Matsumura, K. Tamura, Y. Nishihata,H. Yoshikawa, K. Kobayashi, T. Mori and K. Uosaki, *J. Phys. Chem. C*, 116 (2012) 10098.
190.F. D. Kong, S. Zhang, G. P. Yin, Z. B. Wang, C. Y. Du, G. Y. Chen and N. Zhang, *Int. J. Hydrogen Energy*, 37 (2012) 59.
191.A. Ignaszak, C. Song, W. Zhu, Y. J. Wang, J. Zhang, A. Bauer, R. Baker, V. Neburchilov, S. Ye and S. Campbell, *Electrochem. Acta*, 75 (2012) 220.
192.X. Ma, H. Meng, M. Cai and P. K. Shen, *J. Am. Chem. Soc.*, 134 (2012) 1954.
193.J. Kibsgaard, Y. Gorlin, Z. Chen and T. F. Jaramillo, *J. Am. Chem. Soc.*, 134 (2012) 7758.

194. A. Altamirano-Gutiérrez, A. M. Fernández and F. J. Rodríguez Varela, *Int. J. Hydrogen Energy*, 38 (2013) 12657.
195. G. Fu, K. Wu, J. Lin, Y. Tang, Y. Chen, Y. Zhou and T. Lu, *J. Physical Chemistry C*, 117 (2013) 9826.
196. S. M. Alia, K. Jensen, C. Contreras, F. Garzon, B. Pivovar and Y. Yan, *ACS Catal.*, 3 (2013) 358.
197. S. M. Alia, K. O. Jensen, B. S. Pivovar and Y. Yan, ACS *Catal.*, 2 (2012) 858.